

Review

Recent Developments in Materials for Physical Hydrogen Storage: A Review

Thi Hoa Le ¹, Minsoo P. Kim ², Chan Ho Park ^{1,*} and Quang Nhat Tran ^{1,*}

¹ Department of Chemical and Biological Engineering, Gachon University, 1342 Seongnam-daero, Sujeong-gu, Seongnam-si 13120, Republic of Korea; lehoa290792@gachon.ac.kr

² Department of Chemical Engineering, Sunchon National University, Suncheon 57922, Republic of Korea; mspkim@scnu.ac.kr

* Correspondence: chhopark@gachon.ac.kr (C.H.P.); tran.nhat147@gachon.ac.kr (Q.N.T.)

Abstract: The depletion of reliable energy sources and the environmental and climatic repercussions of polluting energy sources have become global challenges. Hence, many countries have adopted various renewable energy sources including hydrogen. Hydrogen is a future energy carrier in the global energy system and has the potential to produce zero carbon emissions. For the non-fossil energy sources, hydrogen and electricity are considered the dominant energy carriers for providing end-user services, because they can satisfy most of the consumer requirements. Hence, the development of both hydrogen production and storage is necessary to meet the standards of a “hydrogen economy”. The physical and chemical absorption of hydrogen in solid storage materials is a promising hydrogen storage method because of the high storage and transportation performance. In this paper, physical hydrogen storage materials such as hollow spheres, carbon-based materials, zeolites, and metal–organic frameworks are reviewed. We summarize and discuss the properties, hydrogen storage densities at different temperatures and pressures, and the fabrication and modification methods of these materials. The challenges associated with these physical hydrogen storage materials are also discussed.

Keywords: hydrogen; physical hydrogen storage; hollow spheres; carbon-based materials; zeolites; metal–organic frameworks (MOFs)



Citation: Le, T.H.; Kim, M.P.; Park, C.H.; Tran, Q.N. Recent

Developments in Materials for Physical Hydrogen Storage: A Review. *Materials* **2024**, *17*, 666. <https://doi.org/10.3390/ma17030666>

Academic Editors:
Alessandro Dell’Era and Erwin
Ciro Zuleta

Received: 8 December 2023
Revised: 21 January 2024
Accepted: 23 January 2024
Published: 29 January 2024



Copyright: © 2024 by the authors. Licensee MDPI, Basel, Switzerland. This article is an open access article distributed under the terms and conditions of the Creative Commons Attribution (CC BY) license (<https://creativecommons.org/licenses/by/4.0/>).

1. Introduction

Nonrenewable energy sources (fossil fuels) such as coal, oil, and natural gas have been playing an essential role in the global economy for over 150 years. Fossil fuels account for approximately 80% of the global energy demand [1]. However, fossil-fuel sources are expected to be exhausted and will have to be replenished. In addition, the main component of fossil fuels is carbon; therefore, when fossil fuels are burned to generate energy, carbon dioxide is released into the atmosphere, which causes various environmental and climate problems. The rapid growth of the population and economy has resulted in the fast exhaustion of fossil-fuel sources and serious environmental and climate impacts [2,3]. Therefore, governments of many countries are in a race to transform to alternative and renewable energy to secure their own energy sources and contribute to the “net-zero emission” commitment (nZEC). By 2020, more than 110 countries had signed up to achieve the nZEC target by 2050 [4]; China, one of the countries emitting large amounts of carbon dioxides, had committed to achieve this by 2060 [5]. These countries must have a “net zero-energy building” (nZEB) by 2050, which implies that the amount of energy used by a building every year must be equal to the amount of renewable energy generated onsite. “Zero emission” or “carbon neutrality” imply that even though carbon is emitted, the emitted carbon gas is captured and stored elsewhere or utilized for some purpose [6,7]. The use of renewable energy combined with carbon capture–utilization systems can help address the issues of energy deficiency and global warming.

Hydrogen is light, energy-dense, and storable, and it can be produced from fossil fuels, biomass, water, or their combinations [8]. The use of hydrogen energy does not directly produce pollutants or emit greenhouse gases; therefore, hydrogen is considered one of the cleanest energy sources. Hydrogen contributes significantly to achieving zero carbon emissions and can be considered a clean, secure, and affordable energy source of the future [9].

In addition, hydrogen can promote the development and expansion of renewable energy sources such as solar and wind energy, which are not always available to match the demand. Hydrogen is one of the best options for renewable energy transfer and storage as well as the lowest-cost option for long-term electricity storage. Hydrogen and hydrogen-based fuels can transport energy from regions with solar and wind resource abundance to energy-poor regions that are thousands of kilometers away [10,11]. Therefore, many countries are implementing policies and projects that support investments in the hydrogen industry. In addition, hydrogen production and storage technologies can be improved, developed, and scaled up to allow hydrogen to be widely used in the future.

Currently, hydrogen storage remains challenging in hydrogen energy applications. In addition to compressed and liquefied hydrogen, hydrogen storage materials play an important role in promoting widespread applications in the hydrogen industry. Compared with the compression and liquefaction approaches, storage materials can store higher-density hydrogen safely; therefore, systems using these materials can be flexibly operated. Moreover, storage materials are the most suitable for both onboard and stationary applications [12].

Hydrogen storage materials are classified into chemisorption and physisorption types, which have pros and cons. Rationally, hydrogen storage materials need to meet the requirements of abundance, safety, low cost, rapid kinetics, easy handling, suitable thermodynamic properties (reversible hydrogen absorption and desorption), and high gravimetric and volumetric densities of hydrogen [13]. Figure 1 shows the classification of hydrogen storage materials. Chemical storage materials have potential of high energy densities and ease of use, especially liquid-involved systems using similar infrastructure to that of today's gas-line refueling stations. However, the dehydrogenation process is relatively challenging due to several irreversible storage approaches of chemical materials [14]. It is unsuitable with ammonia and other storage compounds due to the production of gaseous pollutants such as nitrogen oxides and carbon oxides. Also, metal hydride storage materials have poor kinetics and insufficient thermodynamic stability, although they can be operated at low pressure and ambient temperature, with a higher volumetric energy density [15]. On the other hand, physical storage system can be categorized into control of conditions (pressure/temperature) and the selection of absorbents. Pressure or temperature-controlled storage systems for hydrogen gas such as cryogenic liquefaction and high-pressure compression technologies have been matured. Nevertheless, they have limitations of safety concerns, high costs, and low storage capacities [16]. The utilization of novel porous materials as a high-throughput hydrogen absorbent in physical hydrogen storage methods point to the future overcoming the critical limitation of today's physical storage system by showing strengths of high storage densities, fast charging–discharging kinetics, and low costs [17]. In this review, we first focus on physical storage absorbents that are used to store compressed hydrogen in a hollow structure or absorb hydrogen in nano- or mesoporous structures such as metal–organic frameworks (MOFs), carbon-based materials, or zeolites.

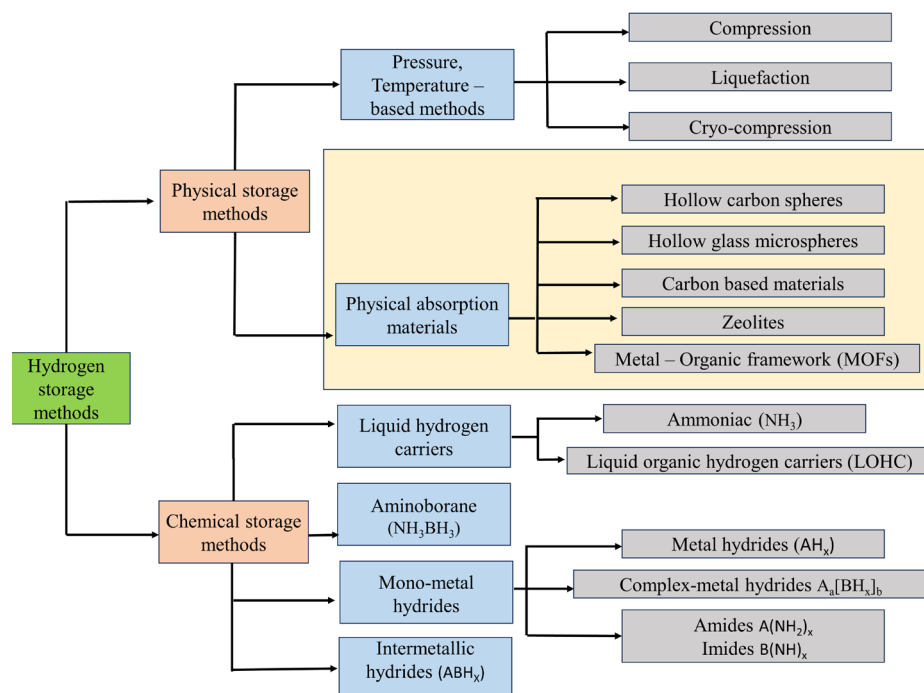


Figure 1. Classification of hydrogen storage materials.

2. Physical Hydrogen Storage Materials

2.1. Compressed Hydrogen Storage Materials

Hydrogen compression is the most widely used technology to storage and utilize hydrogen gas as an energy source with several outstanding advantages [18,19]. First, the compression technique is well developed with hydrogen filling and release occurring at high rates. Moreover, hydrogen release does not require energy [19,20]. Among the various storage materials, hollow spheres are most widely used for compressed hydrogen storage. Hollow spheres not only provide high surface area but also encapsulate hydrogen within pores. Moreover, the high surface area and porosity allow hybridization with other materials via binding sites on the surface or in the pores [21]. Hence, the absorption and catalytic activities of the hollow spheres can be increased significantly. In addition, the good mechanical strength and low specific weight of hollow spheres make them good hydrogen containers [22]. Controlling the different conditions such as reaction time, pH, temperature, and ratio of reactants can simplify the fabrication of hollow spheres of uniform sizes. In hollow nanospheres, hydrogen can be absorbed in both atomic and molecular forms [23].

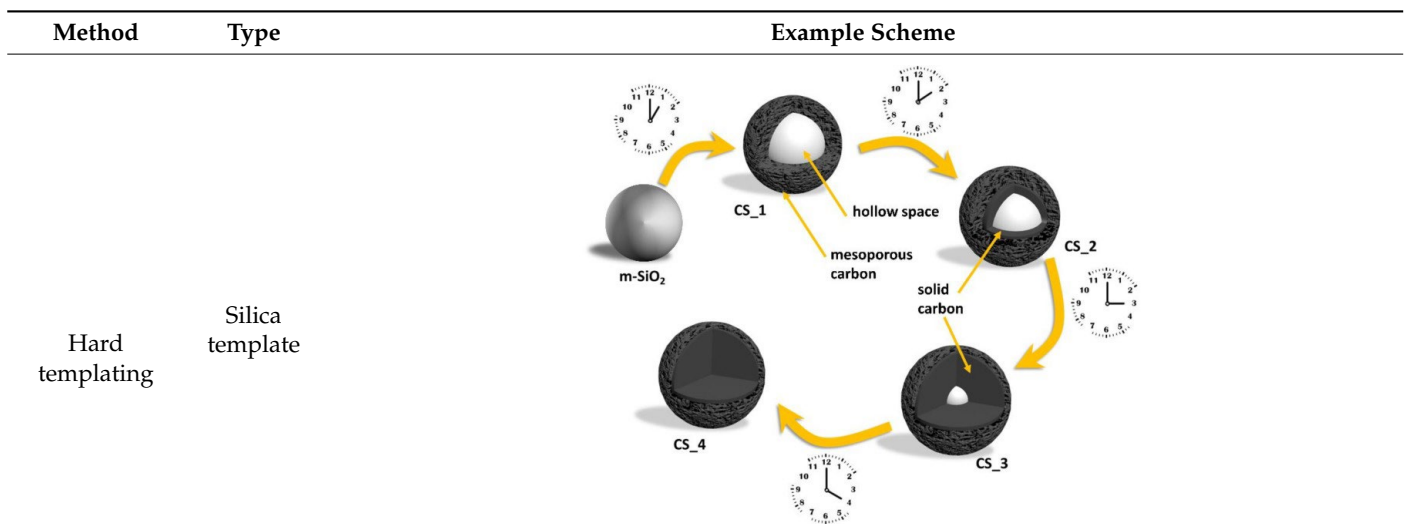
Hollow spheres with average sizes ranging from micrometers to nanometers have attracted considerable research attention. Various types of hollow spheres with different sizes and from different materials including carbon, glass, metal, and nonmetal, have been developed. In this review, we mainly discuss hollow carbon spheres and hollow glass microspheres, which have been attracting considerable attention.

2.1.1. Hollow Carbon Spheres (HCSs)

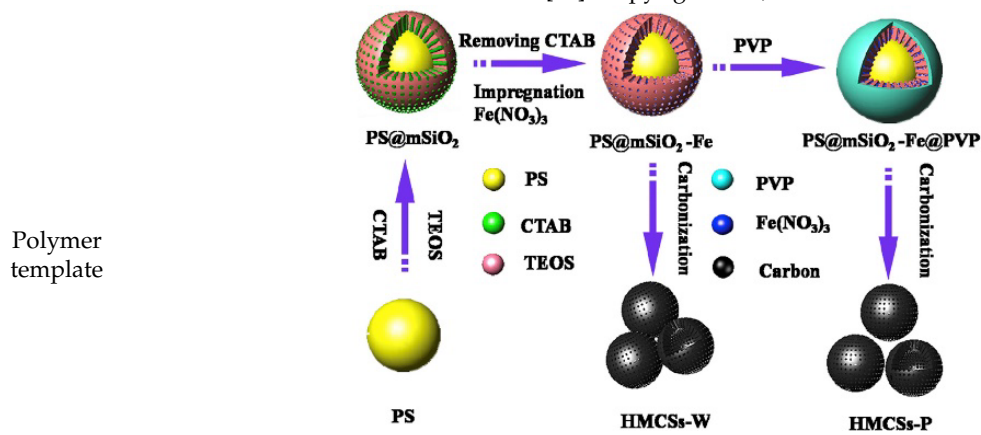
HCSs are mainly fabricated by two methods: hard templating and soft templating, which use different template types to create a hollow sphere (HS). The hard-templating approach employs special hard particles as a “core template” to build a hollow structure. The core is removed after a carbon shell is formed on the surface of the core. Silica, polymers, and hard metal particles are often used as core templates in hard-templating procedures. In soft templating, a hollow structure is directly generated by the self-assembly of carbon and other organic compounds. Hence, the core templates are “soft” precursor molecules, which easily decompose during the final pyrolysis. Table 1 illustrates the formation of HCS via hard (silica, polymer, and metal templating with the example Schemes 1–3, respectively)

and soft (surfactants and organic additives templating with the example Scheme 4 and Scheme 5, respectively). Both approaches have their advantages and disadvantages. Hard templating allows better control of the HCS properties, but it requires considerable time and nonenvironmentally friendly processes to remove the core templates after the shell formation. The template is decomposed easily during soft templating [24]; however, it is more difficult to control the size and morphology of the HCS via soft templating.

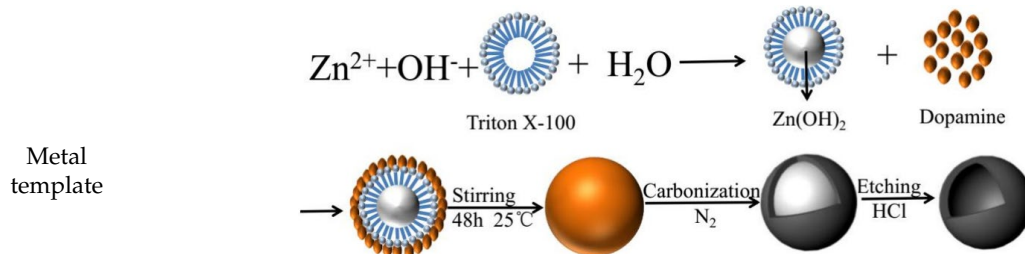
Table 1. Hollow carbon sphere (HCS) synthesis methods.



Scheme 1. Schematic of the formation process of hollow carbon spheres. Reprinted with permission from [25]. Copyright 2018, MDPI.

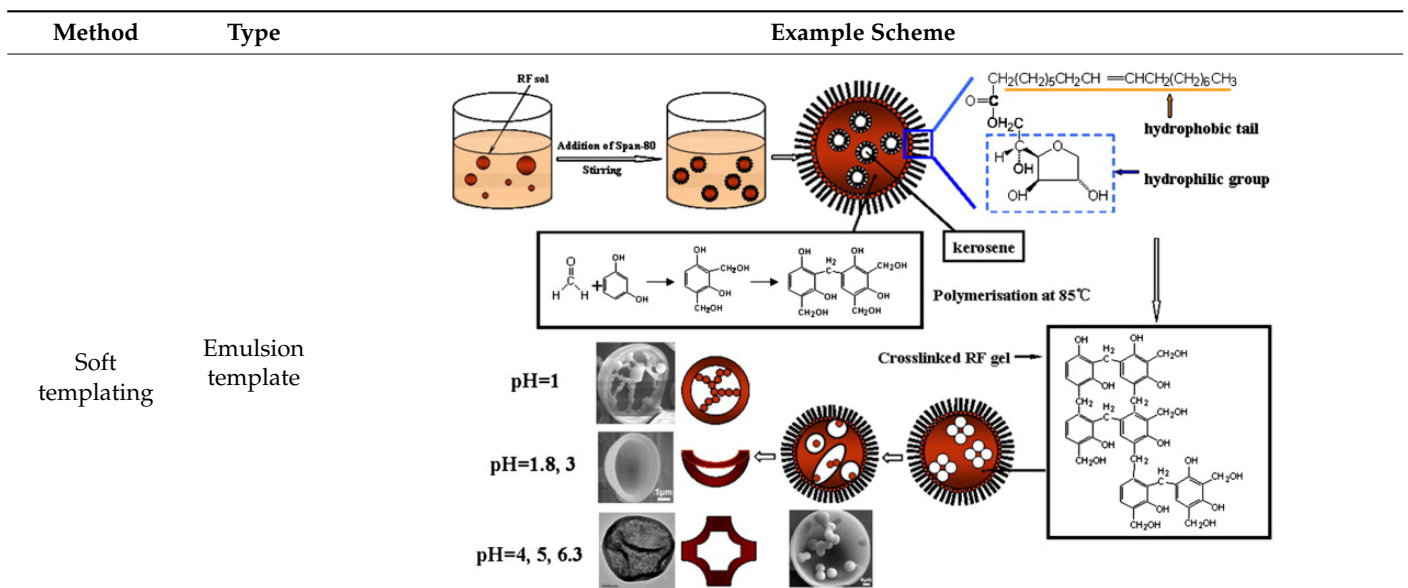


Scheme 2. Illustration of the synthesis route for hollow mesoporous carbon spheres. Reprinted with permission from [26]. Copyright 2018, Elsevier.

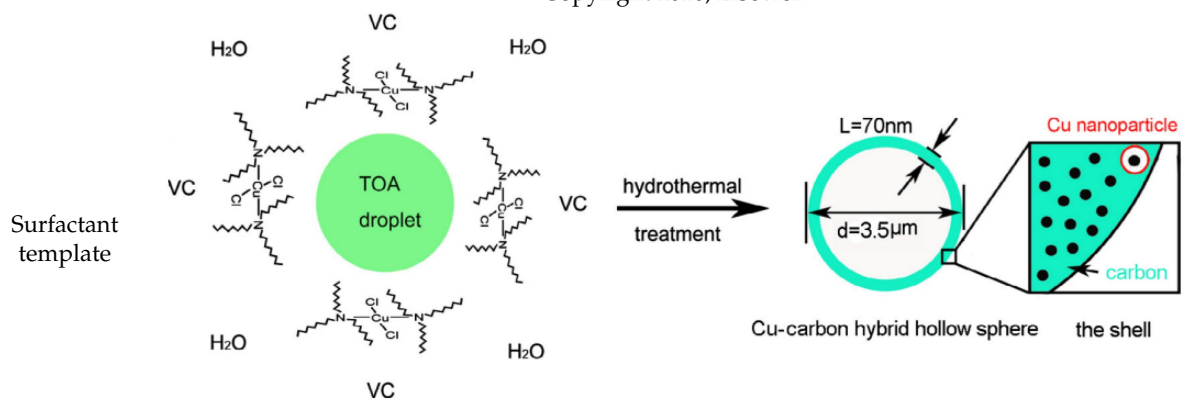


Scheme 3. Schematic of the synthetic process for hollow carbon spheres. Reprinted with permission from [27]. Copyright 2019, Elsevier.

Table 1. Cont.



Scheme 4. Synthesis scheme for carbon hollow particles. Reprinted with permission from [28]. Copyright 2010, Elsevier.



Scheme 5. Formation mechanism of Cu–C hybrid hollow spheres. Reprinted with permission from [29]. Copyright 2013, Elsevier.

HCSs are excellent materials for hydrogen storage. Their mesoporous structure provides a high Brunauer–Emmett–Teller (BET) value, voids, and hollow spaces, which can be occupied by hydrogen; thus, a high hydrogen capacity can be achieved. However, the HCS structure has a significant influence on the hydrogen storage capacity. The shape and size of the HCS play important roles in hydrogen diffusion in the substrate. When the adsorption energy is higher than the release energy, hydrogen can easily occupy the active sites that strongly depend on the morphologies of the material. In addition, the deposition of hydrogen into the pores of the HCS can be facilitated by the defects and thin walls of the HCS; hence, the spaces between the layers can be freed, increasing the amount of hydrogen stored in the HCS [30–32]. Hydrogen storage based on HCS has been reported in several studies, as partly presented in Table 2.

Wu et al. successfully synthesized necklace-like hollow carbon nanospheres (CNSs) with narrow pore distributions using pentagon-containing reactants. The results of their electrochemical hydrogen storage experiments showed that CNSs afforded a capacity of 242 mAh/g at a current density of 200 mA/g, corresponding to a hydrogen storage of 0.89 wt%, which is considerably greater than the electrochemical capacities of solid chain carbon spheres and multiwalled carbon nanotubes [30]. This confirms that the structure and morphology of carbon materials strongly affect the electrochemical hydrogen storage.

Table 2. Various types of HCS used for hydrogen storage.

	Materials	Temperature (°C)	Pressure (bar)	H ₂ Storage Capacity (wt%)	Ave. Particle Size (nm)	Ave. Pore Size (nm)	Total Pore Volume (cm ³ /g)	Surface Area (m ² /g)	Reference
1	Pd-hollow carbon spheres	40	24	0.36	~250	n/a	0.2514–0.9754	147–617	[33]
2	Necklace-like hollow carbon nanospheres (CNS)			0.89	60	5	n/a	594.32	[30]
3	Ni-decorated hollow carbon spheres	25	90	1.23	5100	n/a	0.31	28.6	[34]
4	Hollow nitrogen-containing carbon spheres (N-HCS)	−196	80	1.03	~250	1.38–20	0.84	872	[35]
		25	80	2.21					
5	Fe-nanoparticle-loaded hollow carbon spheres	300	20	5.6	200–500	~90	n/a	160	[36]
6	Metallic Mg ions diffused in hollow carbon nanospheres (HCNS)	270		6.78	440–9800	28	n/a	1810	[37]
		370		7.85					
7	Zeolite-like hollow carbon	−196	1	2.6	~5000	0.6–0.8	~2.41	3200	[38]
		−196	20	8.33					

Doping hollow carbon materials with metals for hydrogen storage is known as hydrogen spillover [39]. Metals doped onto carbon materials can increase the binding energy between hydrogen and the pore walls. In addition, binding can occur between the hydrogen molecules and doped metallic atoms [40]. Thus, metal doping can enhance the hydrogen storage of materials. Among the various metal-doped hollow carbons used for enhancing hydrogen storage, palladium (Pd)-doped carbon materials have been reported to improve the hydrogen storage performance [41–43]. Hydrogen molecules easily dissociate on the Pd surface, which limits the storage efficiency. Hence, to decrease the active surface area of Pd to achieve good catalytic performance and improve the hydrogen storage capacity, small particles of Pd are doped onto the porous surface of the material.

Michalkiewicz et al. synthesized and evaluated the hydrogen storage performance of Pd nanoparticles doped onto HCSs [41]. Their results indicated that the size and amount of Pd nanoparticles significantly affected the hydrogen storage capacity and that size played a more important role than quantity. The small size of the Pd nanoparticles could enhance their cumulative surface area, thereby increasing the spillover effect. With a diameter of 11 nm, the capacity obtained at a temperature of 40 °C and pressure of 24 bar was 0.36 wt%, which was two times higher than the storage capacity of pristine HCSs.

Kim et al. and Jiang et al. reported Ni-loaded HCSs and N-containing HCSs, respectively. Because of their physical sorption characteristics, doping with Ni or N does not affect the hydrogen absorption at ambient temperature [44]. However, the results show that the hydrogen uptake capacities of Ni-loaded HCSs and N-containing HCSs are 1.23 wt% and 2.21 wt%, respectively, at room temperature [34,35]. This is because the dissociation of hydrogen molecules into atomic hydrogen can easily occur in the presence of Ni nanoparticles, following which hydrogen atoms are chemically adsorbed by the sorbents, resulting in an enhanced capacity for storing hydrogen. Moreover, the spillover reaction provided by Ni decoration also enhances the hydrogen storage capacity. For N-doped HCSs, N atoms can activate carriers, create more defect sites, and enhance the hydrogen–carbon binding strength on the carbon surface. Hence, the hydrogen absorption mechanism changes from physisorption to physicochemical adsorption [35,45].

Khaled et al. fabricated Mg ions diffused in hollow carbon nanospheres embedded with platinum nanoparticles (Mg/HCNS/Pt). This material was expected to act as an efficient hydrogen carrier for energy-release applications. At temperatures of 270, 300, 330, and 370 °C, the obtained hydrogen desorption capacities were 6.78, 6.92, 7.05, and

7.85 wt% respectively. The kinetics experiments showed that Mg/HCNS/Pt only took 85.2 and 168 s to release a maximum of 7.85 wt% at 370 °C and minimum of 6.78 wt% desorption capacity at 270 °C, respectively [37]. This study indicated that although doping with metal elements could enhance the hydrogen storage capacity of HCSs, the hydrogen adsorption capacity of this composite material was not suitable for application at ambient temperatures. Improvements in terms of new materials or fabrication techniques are necessary to overcome this limitation.

In addition to metal and nonmetal doping, the hydrogen storage capacity can be enhanced by improving the surface area of the HCS. Yang et al. used chemical vapor deposition to successfully synthesize zeolite-like HC materials with large surface areas. This material demonstrated the effect of surface area on hydrogen storage capacity, which was 2.6 wt% at a pressure of 1 bar and reached 8.33 wt% at a pressure of 20 bar. This capacity of the zeolite HC material was recorded as the highest value ever reported among HC materials.

2.1.2. Hollow Glass Microspheres (HGMs)

HGMs, also known as microballoons or microbubbles, are mainly composed of borosilicate and soda lime silica. The sizes of HGMs range from 100 nm to 5 µm with a wall thickness ranging from 1.5 to 3 µm and pore size from 100 to 500 nm [46,47]. The wall thickness of HGMs strongly determines their crush strength; the higher the sphere density, the higher the crush strength. Owing to their excellent chemical stability, chemical resistance, strong mechanics, low density, high-temperature operation, high water resistance, noncombustibility, nonexplosibility, nontoxicity, and particularly, low-cost production, HGMs are considered as high-potential hydrogen transporting and storing materials [32,33,48].

HGMs must be operated under high pressure and high temperature to enhance the hydrogen diffusion into the HGMs. This is because not only the sizes of the gas molecules but also the temperature can change the gas diffusivity. After hydrogen molecules are absorbed in the HGMs, the temperature must be decreased to room temperature to reduce the diffusivity rate and retain the loaded hydrogen molecules in the pore cavities. For the hydrogen-release process, it is necessary to heat the HGMs to high temperatures. The optimal temperature for both hydrogen absorption and desorption is over 300 °C [49,50].

HGMs can be fabricated using dry-gel or liquid-droplet approaches. The high-temperature furnace in which the initial particles are formed plays an important role in both methods. First, the blowing agent is broken down to release the gas within the dried gel or liquid. The fast growth of gaseous products leads to the appearance of bubbles and the formation of hollow droplets. Thereafter, the hollow droplets rapidly cool from the liquid state to form HGMs [51]. Regarding the synthesis of HGMs, Wang et al. presented a basic formula for a new type of HGM, based on the traditional fabrication approaches, experiences in this material industry, and interrelated businesses. According to their proposal, HGM comprised quartz sand, K₂CO₃, Na₂B₈O₁₃·4H₂O, Na₂CO₃, Ca(OH)₂, NaAlO₂, Li₂CO₃, and H₂O in weight percentages of 27, 14.5, 15, 10, 3.5, 3, 0.5, and 26.5%, respectively. Hence, the main chemical components of HGM were SiO₂ (68–75%), Na₂O (5–15%), CaO (8–15%), B₂O₃ (15–20%), and Al₂O₃ (2–3%) [52].

Dalai et al. presented a type of HGM for hydrogen storage, which was synthesized using an air–acetylene flame spheroidization method using urea as the blowing agent. With a microsphere diameter of 10–200 µm and wall thickness of 0.5–2 µm, they showed hydrogen storage capacity at ambient temperature and at 200 °C under a pressure of 10 bar. The results indicated that the adsorption capacity at ambient temperature was lower than that at 200 °C [53]. This confirmed that the higher the temperature, the better the gas diffusivity. At high temperatures, hydrogen molecules could pass through the HGM walls toward the hollow pores and were retained in them.

The poor thermal conductivity of HGMs restricts hydrogen molecule loading during the absorption and desorption processes, resulting in a poor hydrogen storage capacity [50]. It has been discovered that when HGMs are doped with photoactive agents such as Ti,

Cr, V, Fe, Zn, Mg, and Co, the gas diffusion rate is strongly enhanced by light illumination compared with that of traditional heating furnace approaches [50,54–56]. Figure 2 illustrates photo-induced outgassing in Titanium (Ti) ion-doped HGMs due to light absorption [54]. Particularly, this research investigates the influence of Ti doping on the gas retention capacity and photo-induced outgassing behavior of HGMs. The gas retention capacity of HGMs is of great importance for hydrogen storage. In this study, the gas retention properties of HGMs with different Ti concentrations were investigated through evaluation of their pressure half-life ($t_{1/2}$) and deuterium (D_2) permeability. The discovery of photo-induced hydrogen diffusion through glass-shell HGMs loaded with photoactive metals paves the way for new revolutionary methods for filling, storing, transporting, and releasing hydrogen.

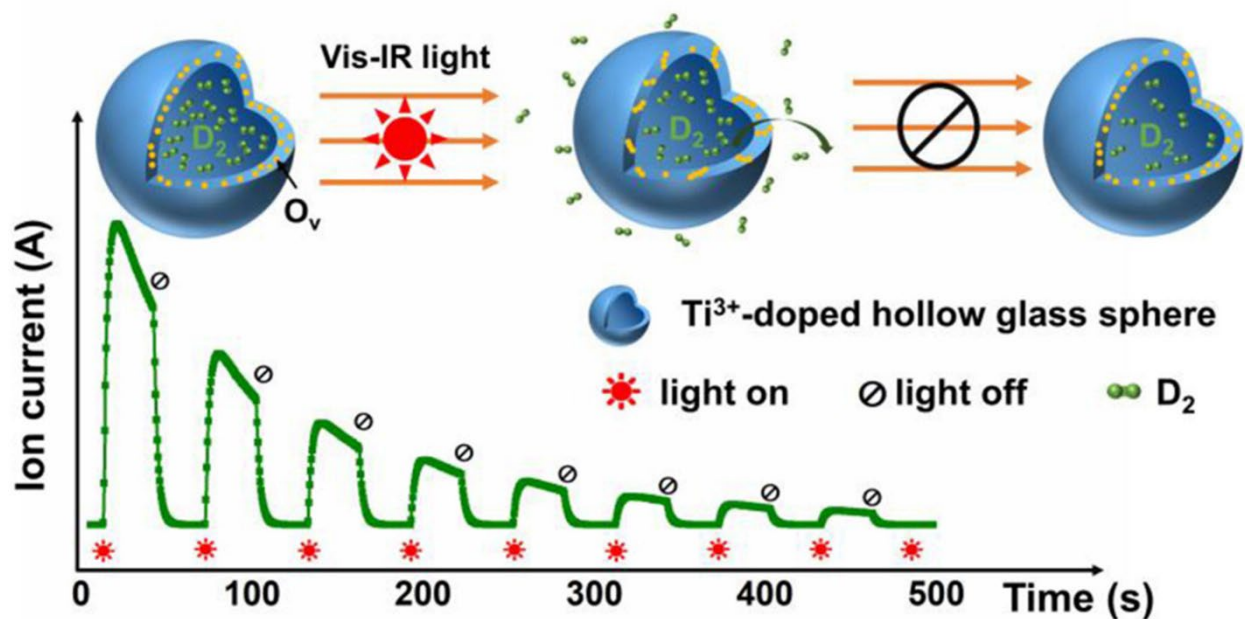


Figure 2. Photo-induced gas release in Ti^{3+} -doped hollow glass microsphere (HGM). Reprinted with permission from [54]. Copyright 2023, Elsevier.

Dalai et al. synthesized HGM samples loaded with Fe and Mg to improve their heat transfer properties, thereby enhancing their hydrogen storage capacity. For Fe doping, the feed glass powder was mixed with certain amounts of ferrous chloride tetrahydrate solution and magnesium nitrate hexahydrate salt solution to obtain 0.2–2 wt% Fe loading and 0.2–3.0 wt% Mg loading, respectively, in the HGMs. Hydrogen adsorption experiments on all HGMs doped with Fe and Mg were performed at 10 bar and 200 °C for 5 h. The results indicated that the hydrogen uptake capacity of Fe-doped HGMs was approximately 0.56 wt% at 0.5 wt% iron loading. Increasing the iron content did not enhance the hydrogen absorption because of spheroidization and the FeO/Fe block, which prevented the accessibility of some pores. This was confirmed by the results of 0.21 wt% uptake capacity with 2 wt% Fe doping in HGMs. Meanwhile, the Mg-doped sample exhibited a hydrogen adsorption increase from 1.23 to 2.0 wt% as the Mg loading percentage increased from 0 to 2.0 wt%. This is similar to the phenomenon of Fe doping; if the amount of Mg in the HGMs was over 2 wt%, nanocrystals of MgO/Mg that could close the pores appeared, thereby decreasing hydrogen storage capacity [57].

Dalai et al. also fabricated HGMs loaded with Zn to improve their thermal conductivities. Figure 3 shows the environmental scanning electron microscopy images of the HGMs doped with various amounts of Zn. The results showed that Zn doping increased the thermal conductivity and pore density of HGMs. The number of pores increased when the amount of zinc rose from 0.5 wt% to 2 wt%, but it was observed that the pore width

decreased. When the zinc concentration was increased to 5 wt% and 10 wt%, most of the small pores were closed, and the pore number was reduced too because the deposition of the ZnO-rich layer blocked the pores in the HGMs [58].

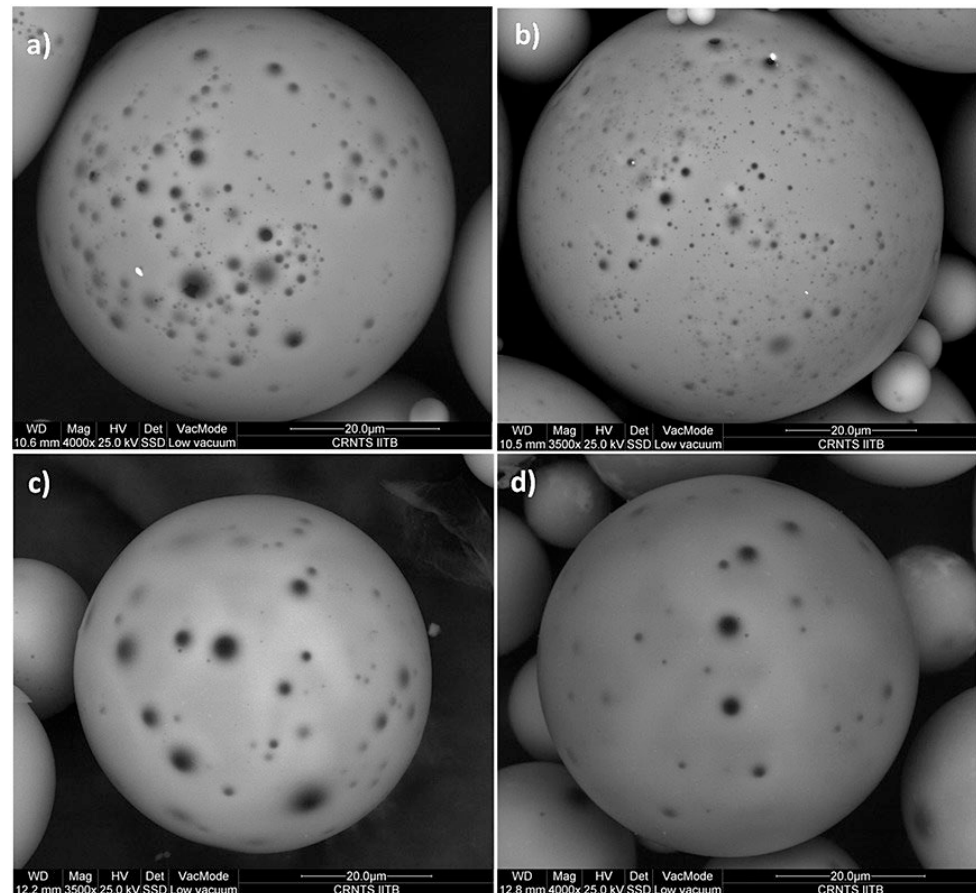


Figure 3. Environmental scanning electron microscopy images of HGMs doped with different amounts of zinc: (a) 0.5, (b) 2, (c) 5, and (d) 10%. Reprinted with permission from [58]. Copyright 2015, Hindawi.

To sum up, the metal doping can increase the porosity of HGMs and then lead to an enhancement in hydrogen storage capacity. However, the too high concentrations of metal can result in the formations of metal oxide layers or the agglomeration metal particles, which can close the pores of HGMs and then decrease the hydrogen loading volume. Hence, doped-metal concentration optimization is extremely crucial to obtain the highest hydrogen storage capacity for HGMs. Overall, we summarize the general characterization of the glass microspheres in Table 3.

Table 3. Summary of characterization of glass microspheres (GMs).

Preparation Method	Types	Advantages	Drawbacks
- Flame synthesis	- Solid GM	- Excellent chemical stability	- Harsh synthetic condition
- Liquid droplet	- Hollow GM	- Chemical resistance	- Fragility: weakness to impact damage
- Dried gel	- Porous GM	- Strong mechanical strength	- Not enough compressive strength
- Electrical arc plasma	- Doped GM	- Low density	- Poor thermal conductivity
		- High thermal stability	- Relatively difficult morphological control
		- High water resistance	- Temperature sensitivity in hydrogen storage
		- Noncombustibility	- Limited hydrogen storage capacity
		- Nonexplosibility	
		- Nontoxicity	
		- Fair cost	

Co-loaded HGMs have also been fabricated [59,60]. The results revealed that the number of pores in the HGMs increased significantly and that the hydrogen storage capacity reached a maximum of approximately 2 wt% at Co concentration ≤ 2 wt%. When the amount of Co exceeded 2 wt%, energy-dispersive spectroscopy (EDS) analysis confirmed the formation of cobalt oxides on the walls of HGMs, which occupied the pores and prevented hydrogen diffusion.

2.2. Physical Absorption Materials

The physical hydrogen absorption process involves loading hydrogen onto the material surface. The origin of this process is the resonant fluctuations in the charge distribution, which are known as dispersive forces or van der Waals interactions. The interaction forces between hydrogen molecules and other materials are quite weak; therefore, physisorption only occurs at temperatures lower than 0 °C [61]. However, because of its advantages of high energy efficiency [46], high rates of loading and unloading [46,62], and good refueling time [63], physisorption has been widely used in the recent years. Hence, absorbent materials have been developed and improved to meet the physisorption requirements. A good hydrogen absorbent depends on two factors: (1) the binding energy between hydrogen molecules and materials, which directly affects the operating temperature of the hydrogen storage system, and (2) the availability of a high average surface area per unit volume [64]. Recently, materials considered excellent candidates for hydrogen physisorption include carbon-based materials such as activated carbon (AC), carbon nanotubes (CNT), graphite nanofibers (GNF), graphene, zeolites, and MOFs, which are further discussed in the following sections.

2.2.1. Carbon-Based Materials

Carbon is one of the most abundant elements in both living and nonliving organisms. Carbon materials are easily prepared as powders with high porosity and have a propensity to interact with gas molecules. Therefore, carbon is a well-known medium capable of absorbing gases and has been used as a detoxifier and purifier.

Carbon-based materials have attracted much attention as promising materials for hydrogen storage because of their several advantages such as high surface area, high porosity with diverse pore structures, good chemical stability, low weight, and low cost [65,66]. Various carbon-based materials are used for hydrogen storage. In this review, we focus on the use of materials such as AC, CNT, GNF, and graphene for hydrogen storage, as summarized in Table 4. Examples of hydrogen storage mechanisms using AC, CNT, GNF, and graphene nanocomposites are shown in Schemes 6–9, respectively (Table 5).

Table 4. Carbon-based materials used in hydrogen storage.

Material	Definition	Advantages	wt% H ₂	T (K)	P (bar)	Ref.
Activated carbon (AC)	Modified synthetic carbon consisting of high-surface-area amorphous carbon and graphite; fabricated through thermal or chemical procedures [67]	High specific surface area Mechanical and chemical stabilities Microporous structure Relatively low cost Feasible commercial scaling [68,69]	0.1	298	10	[70]
			2.02	77		
			0.6	298	120	[71]
			4	77		
			0.85	77	100	[72]
			1.2	298		
			2.7	500	40	[73]
			5.6	77		
			1.09–2.05	298	0.00011	[74]
			5	77	30–60	[75]

Table 4. Cont.

Material	Definition	Advantages	wt% H ₂	T (K)	P (bar)	Ref.			
Carbon nanotubes (CNTs)	CNTs are macromolecules containing a hexagonal arrangement of hybridized carbon atoms, which may be formed by rolling up a single sheet of graphene to form single-walled nanotubes (SWNTs) or multiple sheets of graphene to form multiwalled nanotubes (MWNTs) [76]	Unique structure Narrow size distribution and pore volume High surface area High strength Good electrical conductivity Good mechanical and thermal properties Low density Chemical stability Special functional properties [77–80]	SWNT						
			0.8		30	[81]			
			1.73		77	100	[82]		
			4.77		323		[83]		
			4.77		323		[84]		
			MWNT						
			0.2		298	100	[85]		
			0.54		77	10	[86]		
			1.7		298	120	[87]		
			2			0.05	[88]		
			3.46			127.9	[89]		
			3.8		425	30	[90]		
			Graphite nanofibers (GNFs)	GNFs are produced from the dissociation of carbon-containing gases over a catalyst surface (e.g., metal or alloy) through chemical deposition. The solid consists of very small graphite platelets of width 30–500 Å, stacked in a perfectly arranged conformation [91]	Herringbone structure High degree of defects (exhibits the best performance for hydrogen storage) Several pretreatment procedures: oxidative, reductive, and inert environments [92]	1	300	20	[93]
1.2	77	20				[94]			
3.3	298	48.3				[95]			
4–6.5	298	121.6				[96]			
1.3–7.5	298	100				[97]			
10–15	300	121.16				[98]			
7–10 (irreversible)									
20–30 (reversible)									
Graphene-based materials	Graphene is a monolayer while graphite is a multilayer of carbon atoms strongly bound in a hexagonal crystal lattice. This is a carbon allotrope in the sp ² hybridized form with a molecular bond length of 0.142 nm [99]	High specific surface area High mechanical strength High corrosive-environment resistance High thermal and electrical conductivities [100,101] Various oxygen-containing functional groups				0.055	293	1.06	[102]
						0.13			
			0.14	298	1	[103]			
			1.18		60				
			2.2	298	100	[104]			
			3.3	323		[105]			
			4.3	298	40				
			1	293	120	[106]			
			5	77					
			6.28	298	1.01	[107]			
10.5	77	10	[108]						

Table 5. Examples of hydrogen storage mechanisms of different types of carbon materials.

Carbon Material	Hydrogen Storage Mechanism
Activated carbon	

Scheme 6. Schematic of hydrogen (a) physisorption and (b) chemisorption using activated carbon (AC). Reprinted with permission from [109]. Copyright 2007, Royal Society

Table 5. Cont.

Carbon Material	Hydrogen Storage Mechanism
Carbon nanotube	
Carbon nanofibrous	
Graphene	

Scheme 7. Mechanism of carbon nanotube (CNTs) for hydrogen storage. Reprinted with permission from [110]. Copyright 2020, MDPI

Scheme 8. Ultramicroporous carbon nanofibrous mats for hydrogen storage. Reprinted with permission from [111]. Copyright 2022, American Chemical Society

Scheme 9. (D) Reaction mechanism of hydrogen charging Ca/Graphene nanocomposite. Reprinted with permission from [112]. Copyright 2020, Intechopen

2.2.2. Zeolites

Zeolites are three-dimensional, microporous, and highly crystalline aluminosilicate materials. Zeolites have a tetrahedral framework structure in which Si and Al atoms are tetrahedrally coordinated through shared oxygen atoms. Zeolites are well-known materials with channels and cages in which cations, water, and small molecules can reside. In addition, their high thermal stabilities and good ion-exchange capacities render them a huge potential promising media for hydrogen storage [113,114].

Zeolites can be classified as natural or synthetic. Natural zeolites exhibit improved resistivity and thermal stability in different environments [115]. However, they contain impurities that are not uniform in crystal size; therefore, they cannot be utilized in industrial

applications [116]. In this review, we focus on the synthetic zeolite materials used in the hydrogen storage industry.

Zeolites can be fabricated using various raw materials. To meet the requirements of economic efficiency, the raw materials should be readily available, relatively pure, selective, and inexpensive. Raw materials such as kaolin, rice husk ash, paper sludge, fly ash, blast furnace slag, lithium slag, and municipal solid waste are mostly used for zeolite fabrication.

Zeolites can be synthesized through different approaches including solvothermal, hydrothermal, ionothermal, alkali fusion and leaching, microwave, and ultrasound energy methods, which have been presented in previous studies [116]. Among these approaches, the hydrothermal process is the most widely used, particularly for the synthesis of zeolite membranes [117].

Owing to their excellent properties and various synthetic processes, zeolites are considered as good hydrogen storage candidates. Dong et al. investigated the hydrogen storage capacities of different zeolites including Na-LEV, H-OFF, Na-MAZ, and Li-ABW. The results showed that at a pressure of 1.6 MPa and temperature of 77 K, the capacities of Na-LEV, H-OFF, Na-MAZ, and Li-ABW were 2.07, 1.75, 1.64, and 1.02 wt%, respectively [114]. This result confirms that micropores with a higher volume and diameter, approximating the kinetic diameters of the hydrogen molecules, play a vital role in enhancing the zeolite capacity.

Recently, Sun et al. developed Monte Carlo simulations to predict hydrogen loading under different pressure and temperature conditions for MOFs, hypercrosslinked polymers, and zeolites. Regarding the pressure value, meta-learning allowed the identification of the optimal temperature with the highest working capacity for hydrogen storage. Figure 4 describes the meta-learning system used for the gas uptake prediction. According to this report, the RWY-type and AWO-type zeolites exhibit a hydrogen loading capacity of approximately 7 wt% under a pressure of 100 bar and temperature of 77 K [118].

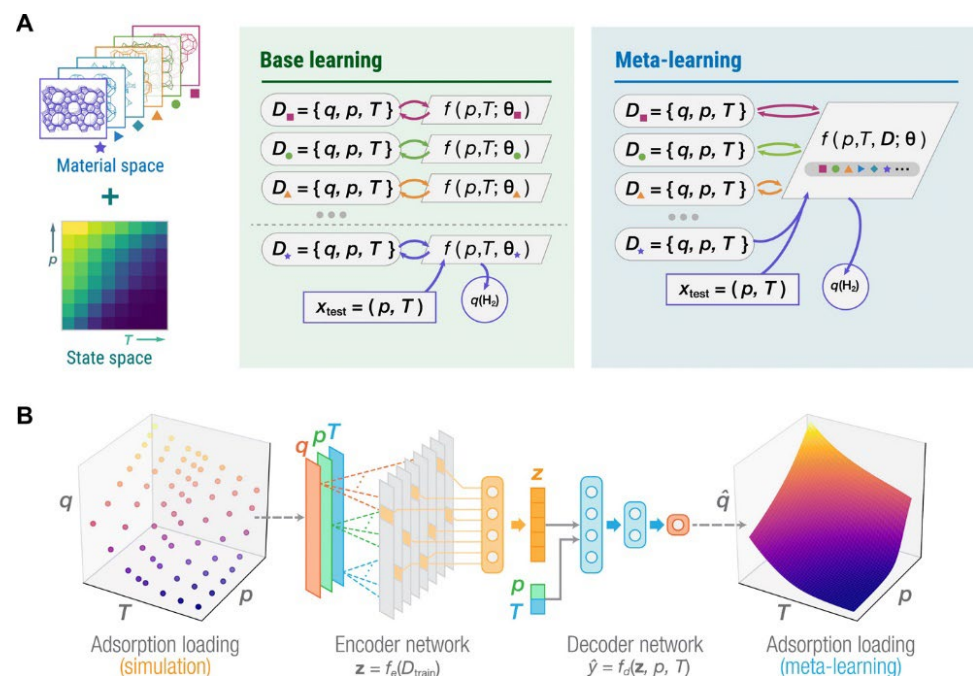


Figure 4. Meta-learning for predicting gas adsorption loading, q , in nanoporous materials. (A) Setup of meta-learning problem. (B) Meta-learning architecture for gas adsorption prediction. Reprinted with permission from [118]. Copyright 2021, American Association for the Advancement of Science.

2.2.3. MOFs

MOFs are an extensive class of crystalline materials that contain metal ions, metal clusters, and organic linkers. Organic linkers such as azoles (1,2,3-triazole, pyrradiazole,

etc.), dicarboxylates (glutaric acid, oxalic acid, succinic acid, malonic acid, etc.), and tricarboxylates (citric acid, trimesic acid, etc.) are commonly used in MOF fabrication [119,120]. In addition to controlling the metal/ligand ratio, changing the reaction temperature and modifying the organic linker are strategies to afford MOFs with good pore structures and high-dimensional frameworks [121], which significantly affect the hydrogen storage capacity. The main hydrogen storage mechanism of MOFs is similar to that of other porous materials such as hollow spheres, carbon-based materials, or zeolites: hydrogen molecules occupy and are kept in their vacants (the pores). The schematic mechanism examples of zeolites and MOFs are described in Figure 5.

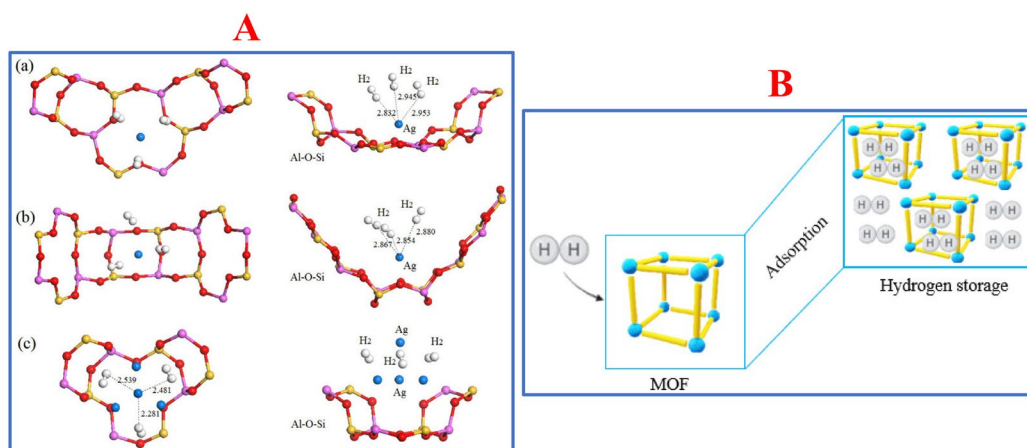


Figure 5. (A) Hydrogen adsorption of zeolites materials named (a) aAg_{0.29}Li_{0.71}-LSX, (b) bAg_{0.43}Li_{0.57}-LSX, and (c) cAg_{0.29}Li_{0.71}-LSX. Reprinted with permission from [122]. Copyright 2019, MDPI; (B) Scheme of MOFs capturing hydrogen via their adsorbent properties. Reprinted with permission from [123]. Copyright 2022, MDPI.

MOFs materials are excellent candidates for potential applications in clean energy such as media for storing gases such as hydrogen and methane because of their high crystallinity, large internal surface area that can reach up to 6000 m²/g, and ultrahigh porosity with up to 90% free volume [124]. In addition, the variability in the metal and organic components in their structures endows MOFs with good designability, tunable structures, and properties. However, the production of MOFs is quite complex, and the hydrogen uptake efficiency of MOFs at ambient temperature is low. Therefore, improvements in the MOF fabrication technology are necessary [125].

A wide range of MOFs synthesis processes have been developed, which are summarized in Table 6. After synthesis, the MOF material obtained is typically available in a powder form. The incorporation of powders into relevant devices is quite difficult; this can prevent the utilization of MOFs in energy or gas-storage applications [126]. For example, if the MOFs are introduced as a loose powder into a tank with pipe fittings, they may be easily blown off into the surroundings, causing difficulties in handling and contamination in pipe fittings. In addition, their low packing density can compromise the volumetric capacities of the pipe fittings. Scientists have made great efforts to shape MOFs using the techniques presented in Table 6. The choice of the shaping technique depends on the fabrication approach and expected textural properties of the MOF materials [127,128]. Shaped MOF materials with appropriate mechanical strength, low flow resistance, and intact or high secondary surface areas and pore volumes are desired for better hydrogen storage performance [126].

Hydrogen molecules have low polarizability. In addition, interactions between hydrogen and most MOFs are relatively weak. Previous research showed that the isosteric heat of hydrogen absorbed in the highly porous MOFs was approximately -5 kJ/mol because of the weak interactions of hydrogen molecules [125]. Hence, cryogenic temperatures are essential for obtaining reasonable hydrogen capacities in MOFs. We conducted research on

some hydrogen storage MOF materials and made a small statistic, as shown in Table 6. The results indicate that the MOF materials exhibit good hydrogen storage capability at low temperatures. Many research groups synthesized and investigated their MOF materials for hydrogen storage, such as MIL-53 (Cr) modified with Pd-loaded activated carbon (MIL-53 Cr) [129], MIL-101 (Cr) with zeolite-templated carbon ZTC (MIL-101 (Cr)/ZTC) [130], iron-based MOF (Fe-BTT) [131], and Co-based MOF (Co-MOF) [132]. They obtained hydrogen storage capacities of less than 5 wt%. With the improvements in the components and structures of materials, as well as using suitable pressures, the recent MOF materials including Zr-based MOFs (NU-1101, NU-1102, NU-1103), Al-based MOFs (NU-1501-Al) [133], and robust azolate-based MOFs (MFU-4/Li) [134] achieved remarkable increases of 9.1, 9.6, 12.6, 14, and 9.4 wt%, respectively, in hydrogen storage capacities.

Table 6. Various synthesis and powder-shaping methods for metal–organic framework (MOF) materials.

MOF Synthesis Methods	MOF Powder-Shaping Methods
1. Microwave assisted method	1. Uniaxial pressing
2. Sonochemistry	2. Coating
3. Electrochemistry	3. Foaming
4. Mechanochemistry	4. Templating
5. Hydrothermal approach	5. Casting
6. Solvothermal approach	6. Granulation
	7. Extrusion
	8. Pulsed current processing

However, storage at ambient temperatures remains a challenge. To overcome the limitations of the driving ranges in fuel-cell vehicles when using adsorption-based hydrogen storage technology, researchers have been developing different methods to increase the performance of MOF materials at higher temperatures. For example, open metal sites in the framework can act as strong adsorption sites for hydrogen loading at ambient temperatures. Lim et al. synthesized Be-based MOF (Be-BTB) with open metal sites. The Be-BTB material with a high BET surface area of 4400 m²/g presented a hydrogen adsorption capacity of 2.3 wt% at 298 K and 100 bar, which is much higher than that of the previous studies [135]. In addition, doping with metal ions or incorporating carbon-based materials may introduce a hydrogen spillover effect (HSPE) that can improve the hydrogen storage capacity of materials at room temperature. The HSPE is a surface phenomenon in which active hydrogen atoms generated by the dissociation of hydrogen molecules on metal surface migrate to the support surface and take part in the catalytic reaction of substance adsorbed on that site [136,137]. There are two conditions ensuring the HSPE can occur. First, there is the existence of metals capable of adsorbing dissociated hydrogen to convert hydrogen molecules into hydrogen atoms or hydrogen ions. Second, there is the presence of an acceptor for active hydrogen species and a channel and driver for the transfer of reactive hydrogen species [138]. The discovery of the HSPE has opened a new strategy in designing efficient catalysts. Especially, the HSPE has attracted much attention as one of the most potential technologies for enhancing the hydrogen storage performance of porous materials including MOFs at ambient temperature. The capacity of materials with induced hydrogen spillover was approximately five times higher than that of pristine MOFs [139]. Yang and co-workers doped 10 wt% Pt/AC catalysts into isoreticular MOF (IRMOF) materials to form a bridging spillover structure between carbon bridges and hydrogen spillovers, leading to a significant enhancement in the hydrogen storage performance. At 298 K and 100 bar, the hydrogen storage capacities of IRMOF-1 and IRMOF-8 increased from 0.4 to 3 wt% and from 0.5 to 4 wt%, respectively [140,141]. Table 7 summarizes the hydrogen storage capacities of some MOF materials.

Table 7. Summary of hydrogen storage capacities of various MOF materials.

MOF Materials Used for Hydrogen Storage at Low Temperature				
Material	Temperature (K)	Pressure (bar)	H ₂ Storage Capacity (wt%)	Reference
Co-MOF	77	1	1.62	[132]
MIL-53	77	60	1.92	[129]
MIL-101 (Cr)/ZTC	77	1	2.55	[130]
CAU-1	70	1	4	
UBMOF-31	77	60	4.9	[131]
Fe-BTT	77	Low Pressure	2.3	[142]
	87		1.6	
	77		95	
NOTT-400	77	1	2.14	[143]
		20	3.84	
NOTT-401	77	1	2.31	[143]
		20	4.44	
NU-1101	77–160	100–5	9.1	[144]
NU-1102	77–160	100–5	9.6	
NU-1103	77–160	100–5	12.6	
NPF-200	77	100–5	8.7	[145]
NU-1500	77–160	100–5	8.2	[146]
NU-1501-Al	77–160	100–5	14	[133]
MFU-4/Li	77–160	100–5	9.4	[134]
MOF materials used for hydrogen storage at ambient temperature				
Material	Temperature (K)	Pressure (bar)	H ₂ storage capacity (wt%)	Reference
HKUST-1	298	65	0.35	[147]
Cu-BTC	303	35	0.47	[148]
HKUST-1	303	35	0.47	[149]
CB/Pt/MOF-5	298	100	0.62	[150]
Zn ₂ (dobpdc)MOFs	298	100	1.3	[151]
Mg ₂ (dobpdc)MOFs	298	100	1.8	
Pd-CNMS/MOF-5	298	100	1.8	[152]
		75	1.6	
		50	1.4	
Be-BTB	298	100	2.3	[135]
V ₂ Cl _{2.8}	298	100	1.64	[153]
NU-150I-Al	296	100	2.9	
IRMOF-1	298	100	3	[140]
IRMOF-8	298	100	4	[120]

2.3. Advantages and Disadvantages of Physical Hydrogen Storage Materials

Hydrogen storage technologies play an extremely important role in the “hydrogen economy”. It is necessary to continuously improve and develop storage materials for the hydrogen industry. As mentioned in the Introduction section, compared to chemical storage materials, the outstanding properties (Table 8) of the physical absorbents and the fact that they do not release greenhouse gases facilitate the global energy transition proceeding effectively as well as achieving the global “net zero emission” target sooner. However, each physical material has both its strength and weakness. The limitations of these materials presented in Table 8 are still challenges in practical hydrogen storage applications.

Table 8. Advantages and disadvantages of physical hydrogen storage materials.

Material	Property	Prospects	Consequences
Hollow spheres		- High surface areas	- Cryogenic temperatures
		- High binding sites	- Agglomeration
		- High gravimetric energy density	- Low volumetric energy density
		- Inexpensive manufacturing process	- Heating requirements for loading and unloading
		- Safety	- Energy cost
		- Scalable possibility	
Carbon-based materials		- Chemical stability	- Pore size uniformity
		- Good thermal	- Binding site deficiency
		- Simple processibility	- Pore structure control
		- Non-expensive	
Zeolites		- Good crystallinity	- Binding site deficiency
		- Hydrolytic and thermal stability	- Low gravimetric loading
		- Non-expensive	- Tunability
		- Structural diversity limitation	
MOFs		- High surface area	- Low hydrogen loading at room temperature
		- High pore volume	- Fabrication process
		- Good crystallinity	
		- Tunability	
		- Design control possibility	
		- Rich metal sites	

3. Conclusions and Recommendation

Materials for physical hydrogen storage such as hollow spheres, carbon-based materials, zeolites, and MOFs exhibit high hydrogen storage densities at cryogenic temperatures. Due to their limitation, they are capable of being utilized only at relatively low tempera-

tures; thus, physical hydrogen storage materials are difficult to use in practical applications compared with that of chemical hydrogen storage materials such as aminoborane complex, liquid organic hydrogen, and metal hydrides at present. Significant efforts have been made to overcome these limitations. For example, certain carbon-based materials, zeolites, and modified MOFs exhibit significantly enhanced hydrogen densities at ambient temperatures. Still, to address these drawbacks and meet the requirements of commercial applications, further research and technical developments are necessary to obtain higher volumetric and gravimetric hydrogen densities. Nevertheless, the effort in developing next-generation materials for physical hydrogen storage should be continued to achieve fast and safe storage of the pure form of hydrogen. In order to open the hydrogen energy-based era in the future, various methodological combinations, as well as existing chemical hydrogen storage methods, will inevitably be required. Then, this physical hydrogen storage material and related methodologies are expected to be in the spotlight as an essential building block.

Author Contributions: Conceptualization, Q.N.T.; methodology, T.H.L.; validation, C.H.P.; formal analysis, T.H.L.; investigation, T.H.L.; resources, Q.N.T.; writing—original draft preparation, T.H.L.; writing—review and editing, T.H.L., M.P.K. and Q.N.T.; supervision, C.H.P. All authors have read and agreed to the published version of the manuscript.

Funding: This work was supported by the Technology Development Program of MSS (RS-2023-00281725) and the ICT Development R&D Program of MSIT (RS-2023-00251670).

Institutional Review Board Statement: Not applicable.

Informed Consent Statement: Not applicable.

Data Availability Statement: No new data were created.

Conflicts of Interest: The authors declare no conflicts of interest.

References

1. Ahmad, T.; Zhang, D. A Critical Review of Comparative Global Historical Energy Consumption and Future Demand: The Story Told so Far. *Energy Rep.* **2020**, *6*, 1973–1991. [[CrossRef](#)]
2. Friedemann, A. *Life after Fossil Fuels. A Reality Check on Alternative Energy*; Lecture Notes in Energy; Springer: Cham, Switzerland, 2021.
3. Hansen, J.; Sato, M.; Kharecha, P.; von Schuckmann, K.; Beerling, D.J.; Cao, J.; Marcott, S.; Masson-Delmotte, V.; Prather, M.J.; Rohling, E.J.; et al. Young People’s Burden: Requirement of Negative CO₂ Emissions. *Earth Syst. Dyn.* **2017**, *8*, 577–616. [[CrossRef](#)]
4. Holechek, J.L.; Geli, H.M.E.; Sawalhah, M.N.; Valdez, R. A Global Assessment: Can Renewable Energy Replace Fossil Fuels by 2050? *Sustainability* **2022**, *14*, 4792. [[CrossRef](#)]
5. Sun, L.-L.; Cui, H.-J.; Ge, Q.-S. Will China Achieve Its 2060 Carbon Neutral Commitment from the Provincial Perspective? *Adv. Clim. Chang. Res.* **2022**, *13*, 169–178. [[CrossRef](#)]
6. Shen, M.; Kong, F.; Tong, L.; Luo, Y.; Yin, S.; Liu, C.; Zhang, P.; Wang, L.; Chu, P.K.; Ding, Y. Carbon Capture and Storage (CCS): Development Path Based on Carbon Neutrality and Economic Policy. *Carbon Neutrality* **2022**, *1*, 37. [[CrossRef](#)]
7. Fankhauser, S.; Smith, S.M.; Allen, M.; Axelsson, K.; Hale, T.; Hepburn, C.; Kendall, J.M.; Khosla, R.; Lezaun, J.; Mitchell-Larson, E.; et al. The Meaning of Net Zero and How to Get It Right. *Nat. Clim. Chang.* **2022**, *12*, 15–21. [[CrossRef](#)]
8. Megía, P.J.; Vizcaíno, A.J.; Calles, J.A.; Carrero, A. Hydrogen Production Technologies: From Fossil Fuels toward Renewable Sources. A Mini Review. *Energy Fuels* **2021**, *35*, 16403–16415. [[CrossRef](#)]
9. Osman, A.I.; Mehta, N.; Elgarahy, A.M.; Hefny, M.; Al-Hinai, A.; Al-Muhtaseb, A.H.; Rooney, D.W. Hydrogen Production, Storage, Utilisation and Environmental Impacts: A Review. *Environ. Chem. Lett.* **2022**, *20*, 153–188. [[CrossRef](#)]
10. Marouani, I.; Guesmi, T.; Alshammari, B.M.; Alqunun, K.; Alzamil, A.; Alturki, M.; Hadj Abdallah, H. Integration of Renewable-Energy-Based Green Hydrogen into the Energy Future. *Processes* **2023**, *11*, 2685. [[CrossRef](#)]
11. Nadaleti, W.C.; dos Santos, G.B.; Lourenço, V.A. Integration of Renewable Energies Using the Surplus Capacity of Wind Farms to Generate H₂ and Electricity in Brazil and in the Rio Grande Do Sul State: Energy Planning and Avoided Emissions within a Circular Economy. *Int. J. Hydrog. Energy* **2020**, *45*, 24190–24202. [[CrossRef](#)]
12. Hirscher, M.; Yartys, V.A.; Baricco, M.; Bellosta von Colbe, J.; Blanchard, D.; Bowman, R.C.; Broom, D.P.; Buckley, C.E.; Chang, F.; Chen, P.; et al. Materials for Hydrogen-Based Energy Storage—Past, Recent Progress and Future Outlook. *J. Alloys Compd.* **2020**, *827*, 153548. [[CrossRef](#)]
13. Kojima, Y.; Miyaoka, H.; Ichikawa, T. Chapter 5—Hydrogen Storage Materials. In *New and Future Developments in Catalysis*; Suib, S.L., Ed.; Elsevier: Amsterdam, The Netherlands, 2013; pp. 99–136. ISBN 978-0-444-53880-2.

14. Suárez, S.H.; Chabane, D.; N'Diaye, A.; Ait-Amirat, Y.; Djerdir, A. Feasibility of Efficiency Improvement in a Fuel Cell System Powered by a Metal Hydride Tank. In Proceedings of the IECON 2022—48th Annual Conference of the IEEE Industrial Electronics Society, Brussels, Belgium, 17–20 October 2022; pp. 1–6.
15. Kojima, Y. Hydrogen Storage Materials for Hydrogen and Energy Carriers. *Int. J. Hydrog. Energy* **2019**, *44*, 18179–18192. [[CrossRef](#)]
16. Zhang, L. Hydrogen Storage Methods, Systems and Materials. *Highlights Sci. Eng. Technol.* **2023**, *58*, 371–378. [[CrossRef](#)]
17. Lee, S.-Y.; Lee, J.-H.; Kim, Y.-H.; Kim, J.-W.; Lee, K.-J.; Park, S.-J. Recent Progress Using Solid-State Materials for Hydrogen Storage: A Short Review. *Processes* **2022**, *10*, 304. [[CrossRef](#)]
18. Durbin, D.J.; Malardier-Jugroot, C. Review of Hydrogen Storage Techniques for on Board Vehicle Applications. *Int. J. Hydrog. Energy* **2013**, *38*, 14595–14617. [[CrossRef](#)]
19. Zhang, F.; Zhao, P.; Niu, M.; Maddy, J. The Survey of Key Technologies in Hydrogen Energy Storage. *Int. J. Hydrog. Energy* **2016**, *41*, 14535–14552. [[CrossRef](#)]
20. Jensen, J.O.; Vestbø, A.P.; Li, Q.; Bjerrum, N.J. The Energy Efficiency of Onboard Hydrogen Storage. *J. Alloys Compd.* **2007**, *446–447*, 723–728. [[CrossRef](#)]
21. Gröger, H.; Kind, C.; Leidinger, P.; Roming, M.; Feldmann, C. Nanoscale Hollow Spheres: Microemulsion-Based Synthesis, Structural Characterization and Container-Type Functionality. *Materials* **2010**, *3*, 4355–4386. [[CrossRef](#)] [[PubMed](#)]
22. Lou, X.W.; Archer, L.A.; Yang, Z. Hollow Micro-/Nanostructures: Synthesis and Applications. *Adv. Mater.* **2008**, *20*, 3987–4019. [[CrossRef](#)]
23. Gupta, A.; Shervani, S.; Amaladasse, F.; Sivakumar, S.; Balani, K.; Subramaniam, A. Enhanced Reversible Hydrogen Storage in Nickel Nano Hollow Spheres. *Int. J. Hydrog. Energy* **2019**, *44*, 22032–22038. [[CrossRef](#)]
24. Li, S.; Pasc, A.; Fierro, V.; Celzard, A. Hollow Carbon Spheres, Synthesis and Applications—A Review. *J. Mater. Chem. A* **2016**, *4*, 12686–12713. [[CrossRef](#)]
25. Kukułka, W.; Wenelska, K.; Baca, M.; Chen, X.; Mijowska, E. From Hollow to Solid Carbon Spheres: Time-Dependent Facile Synthesis. *Nanomaterials* **2018**, *8*, 861. [[CrossRef](#)] [[PubMed](#)]
26. Wang, G.; Liang, K.; Liu, L.; Yu, Y.; Hou, S.; Chen, A. Fabrication of Monodisperse Hollow Mesoporous Carbon Spheres by Using “Confined Nanospace Deposition” Method for Supercapacitor. *J. Alloys Compd.* **2018**, *736*, 35–41. [[CrossRef](#)]
27. Dong, C.; Li, Z.; Zhang, L.; Li, G.; Yao, H.; Wang, J.; Liu, Q.; Li, Z. Synthesis of Hollow Carbon Spheres from Polydopamine for Electric Double Layered Capacitors Application. *Diam. Relat. Mater.* **2019**, *92*, 32–40. [[CrossRef](#)]
28. Zhang, H.; Ye, F.; Xu, H.; Liu, L.; Guo, H. Synthesis of Carbon Hollow Particles by a Simple Inverse-Emulsion Method. *Mater. Lett.* **2010**, *64*, 1473–1475. [[CrossRef](#)]
29. Jia, B.; Qin, M.; Zhang, Z.; Chu, A.; Zhang, L.; Liu, Y.; Lu, H.; Qu, X. One-Pot Synthesis of Cu–Carbon Hybrid Hollow Spheres. *Carbon* **2013**, *62*, 472–480. [[CrossRef](#)]
30. Wu, C.; Zhu, X.; Ye, L.; OuYang, C.; Hu, S.; Lei, L.; Xie, Y. Necklace-like Hollow Carbon Nanospheres from the Pentagon-Including Reactants: Synthesis and Electrochemical Properties. *Inorg. Chem.* **2006**, *45*, 8543–8550. [[CrossRef](#)]
31. Fang, B.; Kim, M.; Kim, J.H.; Yu, J.-S. Controllable Synthesis of Hierarchical Nanostructured Hollow Core/Mesopore Shell Carbon for Electrochemical Hydrogen Storage. *Langmuir* **2008**, *24*, 12068–12072. [[CrossRef](#)] [[PubMed](#)]
32. Jurewicz, K.; Frackowiak, E.; Béguin, F. Towards the Mechanism of Electrochemical Hydrogen Storage in Nanostructured Carbon Materials. *Appl. Phys. A* **2004**, *78*, 981–987. [[CrossRef](#)]
33. Michalkiewicz, B.; Tang, T.; Kalenczuk, R.; Chen, X.; Mijowska, E. In Situ Deposition of Pd Nanoparticles with Controllable Diameters in Hollow Carbon Spheres for Hydrogen Storage. *Int. J. Hydrog. Energy* **2013**, *38*, 16179–16184. [[CrossRef](#)]
34. Kim, J.; Han, K.-S. Ni Nanoparticles-Hollow Carbon Spheres Hybrids for Their Enhanced Room Temperature Hydrogen Storage Performance. *Trans. Korean Hydrog. New Energy Soc.* **2013**, *24*, 550–557. [[CrossRef](#)]
35. Jiang, J.; Gao, Q.; Zheng, Z.; Xia, K.; Hu, J. Enhanced Room Temperature Hydrogen Storage Capacity of Hollow Nitrogen-Containing Carbon Spheres. *Int. J. Hydrog. Energy* **2010**, *35*, 210–216. [[CrossRef](#)]
36. Soni, P.K.; Bhatnagar, A.; Shaz, M.A. Enhanced Hydrogen Properties of MgH₂ by Fe Nanoparticles Loaded Hollow Carbon Spheres. *Int. J. Hydrog. Energy* **2023**, *48*, 17970–17982. [[CrossRef](#)]
37. Elsabawy, K.M.; Fallatah, A.M. Over Saturated Metallic-Mg-Ions Diffused Hollow Carbon Nano-Spheres/Pt for Ultrahigh-Performance Hydrogen Storage. *Mater. Lett.* **2018**, *221*, 139–142. [[CrossRef](#)]
38. Yang, Z.; Xia, Y.; Mokaya, R. Enhanced Hydrogen Storage Capacity of High Surface Area Zeolite-like Carbon Materials. *J. Am. Chem. Soc.* **2007**, *129*, 1673–1679. [[CrossRef](#)] [[PubMed](#)]
39. Chung, T.-Y.; Tsao, C.-S.; Tseng, H.-P.; Chen, C.-H.; Yu, M.-S. Effects of Oxygen Functional Groups on the Enhancement of the Hydrogen Spillover of Pd-Doped Activated Carbon. *J. Colloid Interface Sci.* **2015**, *441*, 98–105. [[CrossRef](#)]
40. Ramos-Castillo, C.M.; Reveles, J.U.; Zope, R.R.; de Coss, R. Palladium Clusters Supported on Graphene Monovacancies for Hydrogen Storage. *J. Phys. Chem. C* **2015**, *119*, 8402–8409. [[CrossRef](#)]
41. Zielinska, B.; Michalkiewicz, B.; Chen, X.; Mijowska, E.; Kalenczuk, R.J. Pd Supported Ordered Mesoporous Hollow Carbon Spheres (OMHCS) for Hydrogen Storage. *Chem. Phys. Lett.* **2016**, *647*, 14–19. [[CrossRef](#)]
42. Rangel, E.; Sansores, E. Theoretical Study of Hydrogen Adsorption on Nitrogen Doped Graphene Decorated with Palladium Clusters. *Int. J. Hydrog. Energy* **2014**, *39*, 6558–6566. [[CrossRef](#)]
43. Adams, B.D.; Ostrom, C.K.; Chen, S.; Chen, A. High-Performance Pd-Based Hydrogen Spillover Catalysts for Hydrogen Storage. *J. Phys. Chem. C* **2010**, *114*, 19875–19882. [[CrossRef](#)]

44. Pacuła, A.; Mokaya, R. Layered Double Hydroxides as Templates for Nanocasting Porous N-Doped Graphitic Carbons via Chemical Vapour Deposition. *Microporous Mesoporous Mater.* **2007**, *106*, 147–154. [[CrossRef](#)]
45. Zubizarreta, L.; Arenillas, A.; Pis, J.J. Carbon Materials for H₂ Storage. *Int. J. Hydrog. Energy* **2009**, *34*, 4575–4581. [[CrossRef](#)]
46. Lim, K.L.; Kazemian, H.; Yaakob, Z.; Wan Daud, W. Solid-State Materials and Methods for Hydrogen Storage: A Critical Review. *Chem. Eng. Technol.* **2010**, *33*, 213–226. [[CrossRef](#)]
47. Shetty, S.; Hall, M. Facile Production of Optically Active Hollow Glass Microspheres for Photo-Induced Outgassing of Stored Hydrogen. *Fuel Energy Abstr.* **2011**, *36*, 9694–9701. [[CrossRef](#)]
48. Dresselhaus, M.S.; Thomas, I.L. Alternative Energy Technologies. *Nature* **2001**, *414*, 332–337. [[CrossRef](#)]
49. Snyder, M.; Wachtel, P.; Hall, M.; Shelby, J. Photo-Induced Hydrogen Diffusion in Cobalt-Doped Hollow Glass Microspheres. *Phys. Chem. Glas.-Eur. J. Glas. Sci. Technol. Part B* **2009**, *50*, 113–118.
50. Rapp, D.B.; Shelby, J.E. Photo-Induced Hydrogen Outgassing of Glass. *J. Non. Cryst. Solids* **2004**, *349*, 254–259. [[CrossRef](#)]
51. Ouyang, L.; Chen, K.; Jiang, J.; Yang, X.S.; Zhu, M. Hydrogen Storage in Light-Metal Based Systems: A Review. *J. Alloys Compd.* **2020**, *829*, 154597. [[CrossRef](#)]
52. Wang, H.; Wang, Z.; Li, J.; Sun, J.; Wang, T.; Li, W. Research on the Preparation and Performances of a New Type of Hollow Glass Microspheres. *IOP Conf. Ser. Earth Environ. Sci.* **2021**, *821*, 12010. [[CrossRef](#)]
53. Dalai, S.; Vijayalakshmi, S.; Shrivastava, P.; Sivam, S.P.; Sharma, P. Preparation and Characterization of Hollow Glass Microspheres (HGMs) for Hydrogen Storage Using Urea as a Blowing Agent. *Microelectron. Eng.* **2014**, *126*, 65–70. [[CrossRef](#)]
54. Li, F.; Zhou, Y.; Li, B.; Zhang, Z. Permeation and Photo-Induced Outgassing of Deuterium in Hollow Glass Microspheres Doped with Titanium. *Int. J. Hydrog. Energy* **2024**, *49*, 303–313. [[CrossRef](#)]
55. Li, F.; Li, J.; Feng, J.; Zhang, Z.; Li, B. Influence of Titanium Doping on the Structure and Properties of Hollow Glass Microspheres for Inertial Confinement Fusion. *J. Non. Cryst. Solids* **2016**, *436*, 22–28. [[CrossRef](#)]
56. Yu, Y.; Kimura, K. Preparation of V or W Doped TiO₂ Coating Hollow Glass Spheres and Photocatalytic Characterization. *J.-Min. Mater. Process. Inst. Jpn.* **2002**, *118*, 206–210. [[CrossRef](#)]
57. Dalai, S.; Vijayalakshmi, S.; Sharma, P.; Choo, K.Y. Magnesium and Iron Loaded Hollow Glass Microspheres (HGMs) for Hydrogen Storage. *Int. J. Hydrog. Energy* **2014**, *39*, 16451–16458. [[CrossRef](#)]
58. Dalai, S.; Savithri, V.; Shrivastava, P.; Sivam, S.; Sharma, P. Fabrication of Zinc-Loaded Hollow Glass Microspheres (HGMs) for Hydrogen Storage. *Int. J. Energy Res.* **2015**, *39*, 717–726. [[CrossRef](#)]
59. Dalai, S.; Savithri, V.; Sharma, P. Investigating the Effect of Cobalt Loading on Thermal Conductivity and Hydrogen Storage Capacity of Hollow Glass Microspheres (HGMs). *Mater. Today Proc.* **2017**, *4*, 11608–11616. [[CrossRef](#)]
60. Dalai, S.; Vijayalakshmi, S.; Shrivastava, P.; Sivam, S.; Sharma, P. Effect of Co Loading on the Hydrogen Storage Characteristics of Hollow Glass Microspheres (HGMs). *Int. J. Hydrog. Energy* **2014**, *39*, 3304–3312. [[CrossRef](#)]
61. Züttel, A. Materials for Hydrogen Storage. *Mater. Today* **2003**, *6*, 24–33. [[CrossRef](#)]
62. Møller, K.T.; Jensen, T.R.; Akiba, E.; Li, H. Hydrogen—A Sustainable Energy Carrier. *Prog. Nat. Sci. Mater. Int.* **2017**, *27*, 34–40. [[CrossRef](#)]
63. Rivard, E.; Trudeau, M.; Zaghbi, K. Hydrogen Storage for Mobility: A Review. *Materials* **2019**, *12*, 1973. [[CrossRef](#)]
64. Bénard, P.; Chahine, R. Storage of Hydrogen by Physisorption on Carbon and Nanostructured Materials. *Scr. Mater.* **2007**, *56*, 803–808. [[CrossRef](#)]
65. Ustinov, E.A.; Gavrilov, V.Y.; Mel'gunov, M.S.; Sokolov, V.V.; Berveno, V.P.; Berveno, A.V. Characterization of Activated Carbons with Low-Temperature Hydrogen Adsorption. *Carbon* **2017**, *121*, 563–573. [[CrossRef](#)]
66. Alhameedi, K.; Hussain, T.; Bae, H.; Jayatilaka, D.; Lee, H.; Karton, A. Reversible Hydrogen Storage Properties of Defect-Engineered C₄N Nanosheets under Ambient Conditions. *Carbon* **2019**, *152*, 344–353. [[CrossRef](#)]
67. Heidarinejad, Z.; Dehghani, M.H.; Heidari, M.; Javedan, G.; Ali, I.; Sillanpää, M. Methods for Preparation and Activation of Activated Carbon: A Review. *Environ. Chem. Lett.* **2020**, *18*, 393–415. [[CrossRef](#)]
68. Blankenship, L.S.; Balahmar, N.; Mokaya, R. Oxygen-Rich Microporous Carbons with Exceptional Hydrogen Storage Capacity. *Nat. Commun.* **2017**, *8*, 1545. [[CrossRef](#)] [[PubMed](#)]
69. Sdanghi, G.; Nicolas, V.; Mozet, K.; Schaefer, S.; Maranzana, G.; Celzard, A.; Fierro, V. A 70 MPa Hydrogen Thermally Driven Compressor Based on Cyclic Adsorption-Desorption on Activated Carbon. *Carbon* **2020**, *161*, 466–478. [[CrossRef](#)]
70. Chang, Y.-M.; Tsai, W.-T.; Li, M.-H. Characterization of Activated Carbon Prepared from Chlorella-Based Algal Residue. *Bioresour. Technol.* **2015**, *184*, 344–348. [[CrossRef](#)] [[PubMed](#)]
71. Akasaka, H.; Takahata, T.; Toda, I.; Ono, H.; Ohshio, S.; Himeno, S.; Kokubu, T.; Saitoh, H. Hydrogen Storage Ability of Porous Carbon Material Fabricated from Coffee Bean Wastes. *Int. J. Hydrog. Energy* **2011**, *36*, 580–585. [[CrossRef](#)]
72. Jin, H.; Lee, Y.S.; Hong, I. Hydrogen Adsorption Characteristics of Activated Carbon. *Catal. Today* **2007**, *120*, 399–406. [[CrossRef](#)]
73. Jordá-Beneyto, M.; Suárez-García, F.; Lozano-Castelló, D.; Cazorla-Amorós, D.; Linares-Solano, A. Hydrogen Storage on Chemically Activated Carbons and Carbon Nanomaterials at High Pressures. *Carbon* **2007**, *45*, 293–303. [[CrossRef](#)]
74. Sharon, M.; Soga, T.; Afre, R.; Sathiyamoorthy, D.; Dasgupta, K.; Bhardwaj, S.; Sharon, M.; Jaybhaye, S. Hydrogen Storage by Carbon Materials Synthesized from Oil Seeds and Fibrous Plant Materials. *Int. J. Hydrog. Energy* **2007**, *32*, 4238–4249. [[CrossRef](#)]
75. Zhou, L.; Zhou, Y.; Sun, Y. Enhanced Storage of Hydrogen at the Temperature of Liquid Nitrogen. *Int. J. Hydrog. Energy* **2004**, *29*, 319–322. [[CrossRef](#)]

76. Lamari, F.; Aoufi, A.; Malbrunot, P.; Levesque, D. Hydrogen Adsorption in the NaA Zeolite: A Comparison Between Numerical Simulations and Experiments. *J. Chem. Phys.* **2000**, *112*, 5991–5999. [[CrossRef](#)]
77. Oriňáková, R.; Oriňák, A. Recent Applications of Carbon Nanotubes in Hydrogen Production and Storage. *Fuel* **2011**, *90*, 3123–3140. [[CrossRef](#)]
78. Fan, Y.-Y.; Kaufmann, A.; Mukasyan, A.; Varma, A. Single- and Multi-Wall Carbon Nanotubes Produced Using the Floating Catalyst Method: Synthesis, Purification and Hydrogen up-Take. *Carbon* **2006**, *44*, 2160–2170. [[CrossRef](#)]
79. Guldi, D.M.; Rahman, G.M.A.; Zerbetto, F.; Prato, M. Carbon Nanotubes in Electron Donor–Acceptor Nanocomposites. *Acc. Chem. Res.* **2005**, *38*, 871–878. [[CrossRef](#)]
80. Kaskun, S.; Akinay, Y.; Kayfeci, M. Improved Hydrogen Adsorption of ZnO Doped Multi-Walled Carbon Nanotubes. *Int. J. Hydrog. Energy* **2020**, *45*, 34949–34955. [[CrossRef](#)]
81. Rashidi, A.M.; Nouralishahi, A.; Khodadadi, A.A.; Mortazavi, Y.; Karimi, A.; Kashefi, K. Modification of Single Wall Carbon Nanotubes (SWNT) for Hydrogen Storage. *Int. J. Hydrog. Energy* **2010**, *35*, 9489–9495. [[CrossRef](#)]
82. Zhao, T.; Ji, X.; Jin, W.; Yang, W.; Li, T. Hydrogen Storage Capacity of Single-Walled Carbon Nanotube Prepared by a Modified Arc Discharge. *Fuller. Nanotub. Carbon Nanostructures* **2017**, *25*, 355–358. [[CrossRef](#)]
83. Silambarasan, D.; Surya, V.J.; Iyakutti, K. Experimental Investigation of Hydrogen Storage in Single Walled Carbon Nanotubes Functionalized with Borane. *Int. J. Hydrog. Energy* **2011**, *36*, 3574–3579. [[CrossRef](#)]
84. Silambarasan, D.; Surya, V.J.; Vasu, V.; Iyakutti, K. Reversible and Reproducible Hydrogen Storage in Single-Walled Carbon Nanotubes Functionalized with Borane. In *Carbon Nanotubes—Recent Progress Rahman*; Rahman, M.M., Asiri, A.M., Eds.; IntechOpen: Rijeka, Croatia, 2018; ISBN 978-1-78923-053-6.
85. Barghi, S.H.; Tsotsis, T.T.; Sahimi, M. Chemisorption, Physisorption and Hysteresis during Hydrogen Storage in Carbon Nanotubes. *Int. J. Hydrog. Energy* **2014**, *39*, 1390–1397. [[CrossRef](#)]
86. Lee, S.-Y.; Park, S.-J. Influence of the Pore Size in Multi-Walled Carbon Nanotubes on the Hydrogen Storage Behaviors. *J. Solid State Chem.* **2012**, *194*, 307–312. [[CrossRef](#)]
87. Liu, C.; Chen, Y.; Wu, C.-Z.; Xu, S.-T.; Cheng, H.-M. Hydrogen Storage in Carbon Nanotubes Revisited. *Carbon* **2010**, *48*, 452–455. [[CrossRef](#)]
88. Mosquera, E.; Diaz-Droguett, D.E.; Carvajal, N.; Roble, M.; Morel, M.; Espinoza, R. Characterization and Hydrogen Storage in Multi-Walled Carbon Nanotubes Grown by Aerosol-Assisted CVD Method. *Diam. Relat. Mater.* **2014**, *43*, 66–71. [[CrossRef](#)]
89. Mosquera-Vargas, E.; Tamayo, R.; Morel, M.; Roble, M.; Díaz-Droguett, D.E. Hydrogen Storage in Purified Multi-Walled Carbon Nanotubes: Gas Hydrogenation Cycles Effect on the Adsorption Kinetics and Their Performance. *Heliyon* **2021**, *7*, e08494. [[CrossRef](#)] [[PubMed](#)]
90. Lin, K.-S.; Mai, Y.-J.; Li, S.-R.; Shu, C.-W.; Wang, C.-H. Characterization and Hydrogen Storage of Surface-Modified Multiwalled Carbon Nanotubes for Fuel Cell Application. *J. Nanomater.* **2012**, *2012*, 939683. [[CrossRef](#)]
91. Chambers, A.; Park, C.; Baker, R.T.K.; Rodriguez, N.M. Hydrogen Storage in Graphite Nanofibers. *J. Phys. Chem. B* **1998**, *102*, 4253–4256. [[CrossRef](#)]
92. Lueking, A.D.; Yang, R.T.; Rodriguez, N.M.; Baker, R.T.K. Hydrogen Storage in Graphite Nanofibers: Effect of Synthesis Catalyst and Pretreatment Conditions. *Langmuir* **2004**, *20*, 714–721. [[CrossRef](#)]
93. Jain, P.; Fonseca, D.A.; Schaible, E.; Lueking, A.D. Hydrogen Uptake of Platinum-Doped Graphite Nanofibers and Stochastic Analysis of Hydrogen Spillover. *J. Phys. Chem. C* **2007**, *111*, 1788–1800. [[CrossRef](#)]
94. Lueking, A.; Pan, L.; Narayanan, D.; Burgess Clifford, C. Effect of Expanded Graphite Lattice in Exfoliated Graphite Nanofibers on Hydrogen Storage. *J. Phys. Chem. B* **2005**, *109*, 12710–12717. [[CrossRef](#)]
95. Huang, C.-W.; Wu, H.-C.; Li, Y.-Y. Hydrogen Storage in Platelet Graphite Nanofibers. *Sep. Purif. Technol.* **2007**, *58*, 219–223. [[CrossRef](#)]
96. Browning, D.J.; Gerrard, M.L.; Lakeman, J.B.; Mellor, I.M.; Mortimer, R.J.; Turpin, M.C. Studies into the Storage of Hydrogen in Carbon Nanofibers: Proposal of a Possible Reaction Mechanism. *Nano Lett.* **2002**, *2*, 201–205. [[CrossRef](#)]
97. Kim, B.-J.; Lee, Y.-S.; Park, S.-J. Preparation of Platinum-Decorated Porous Graphite Nanofibers, and Their Hydrogen Storage Behaviors. *J. Colloid Interface Sci.* **2008**, *318*, 530–533. [[CrossRef](#)]
98. Gupta, B.K.; Srivastava, O.N. High-Yield Production of Graphitic Nanofibers. *Int. J. Hydrog. Energy* **2008**, *33*, 2975–2979. [[CrossRef](#)]
99. Alekseeva, O.K.; Pushkareva, I.V.; Pushkarev, A.S.; Fateev, V.N. Graphene and Graphene-Like Materials for Hydrogen Energy. *Nanotechnolog. Russ.* **2020**, *15*, 273–300. [[CrossRef](#)]
100. Ivanovskii, A.L. Graphene-Based and Graphene-like Materials. *Russ. Chem. Rev.* **2012**, *81*, 571. [[CrossRef](#)]
101. Dhar, P.; Gaur, S.S.; Kumar, A.; Katiyar, V. Cellulose Nanocrystal Templated Graphene Nanoscrolls for High Performance Supercapacitors and Hydrogen Storage: An Experimental and Molecular Simulation Study. *Sci. Rep.* **2018**, *8*, 3886. [[CrossRef](#)]
102. Wei, L.; Mao, Y. Enhanced Hydrogen Storage Performance of Reduced Graphene Oxide Hybrids with Nickel or Its Metallic Mixtures Based on Spillover Mechanism. *Int. J. Hydrog. Energy* **2016**, *41*, 11692–11699. [[CrossRef](#)]
103. Zhou, C.; Szpunar, J.A.; Cui, X. Synthesis of Ni/Graphene Nanocomposite for Hydrogen Storage. *ACS Appl. Mater. Interfaces* **2016**, *8*, 15232–15241. [[CrossRef](#)]
104. Arjunan, A.; Viswanathan, B.; Nandhakumar, V. Heteroatom Doped Multi-Layered Graphene Material for Hydrogen Storage Application. *Graphene* **2016**, *5*, 39–50. [[CrossRef](#)]

105. Muthu, R.N.; Rajashabala, S.; Kannan, R. Facile Synthesis and Characterization of a Reduced Graphene Oxide/Halloysite Nanotubes/Hexagonal Boron Nitride (RGO/HNT/h-BN) Hybrid Nanocomposite and Its Potential Application in Hydrogen Storage. *RSC Adv.* **2016**, *6*, 79072–79084. [[CrossRef](#)]
106. Klechikov, A.G.; Mercier, G.; Merino, P.; Blanco, S.; Merino, C.; Talyzin, A.V. Hydrogen Storage in Bulk Graphene-Related Materials. *Microporous Mesoporous Mater.* **2015**, *210*, 46–51. [[CrossRef](#)]
107. Kag, D.; Luhadiya, N.; Patil, N.D.; Kundalwal, S.I. Strain and Defect Engineering of Graphene for Hydrogen Storage via Atomistic Modelling. *Int. J. Hydrog. Energy* **2021**, *46*, 22599–22610. [[CrossRef](#)]
108. Ao, Z.; Dou, S.; Xu, Z.; Jiang, Q.; Wang, G. Hydrogen Storage in Porous Graphene with Al Decoration. *Int. J. Hydrog. Energy* **2014**, *39*, 16244–16251. [[CrossRef](#)]
109. Edwards, P.; Kuznetsov, V.; David, B. Hydrogen Energy. *Philos. Trans. A Math. Phys. Eng. Sci.* **2007**, *365*, 1043–1056. [[CrossRef](#)]
110. Lyu, J.; Kudiiarov, V.; Lider, A. An Overview of the Recent Progress in Modifications of Carbon Nanotubes for Hydrogen Adsorption. *Nanomaterials* **2020**, *10*, 255. [[CrossRef](#)]
111. Vergara-Rubio, A.; Ribba, L.; Picón Borregales, D.E.; Sapag, K.; Candal, R.; Goyanes, S. Ultramicroporous Carbon Nanofibrous Mats for Hydrogen Storage. *ACS Appl. Nano Mater.* **2022**, *5*, 15353–15361. [[CrossRef](#)]
112. Ngqalakwezi, A.; Nkazi, D.B. Hydrogen Storage: Materials, Kinetics and Thermodynamics. In *Advanced Applications of Hydrogen and Engineering Systems in the Automotive Industry*; Cocco, L., Aziz, M., Eds.; IntechOpen: Rijeka, Croatia, 2020; ISBN 978-1-83968-298-8.
113. Langmi, H.W.; Book, D.; Walton, A.; Johnson, S.R.; Al-Mamouri, M.M.; Speight, J.D.; Edwards, P.P.; Harris, I.R.; Anderson, P.A. Hydrogen Storage in Ion-Exchanged Zeolites. *J. Alloys Compd.* **2005**, *404–406*, 637–642. [[CrossRef](#)]
114. Dong, J.; Wang, X.; Xu, H.; Zhao, Q.; Li, J. Hydrogen Storage in Several Microporous Zeolites. *Int. J. Hydrog. Energy* **2007**, *32*, 4998–5004. [[CrossRef](#)]
115. Georgiev, D.; Bogdanov, B.; Angelova, K.; Markovska, I.; Hristov, Y. Synthetic Zeolites-Structure, Classification, Current Trends In Zeolite Synthesis. In Proceedings of the International Scientific Conference, Stara Zagora, Bulgaria, 4–5 June 2009.
116. Khaleque, A.; Alam, M.M.; Hoque, M.; Mondal, S.; Haider, J.B.; Xu, B.; Johir, M.A.H.; Karmakar, A.K.; Zhou, J.L.; Ahmed, M.B.; et al. Zeolite Synthesis from Low-Cost Materials and Environmental Applications: A Review. *Environ. Adv.* **2020**, *2*, 100019. [[CrossRef](#)]
117. Bowen, T.C.; Noble, R.D.; Falconer, J.L. Fundamentals and Applications of Pervaporation through Zeolite Membranes. *J. Memb. Sci.* **2004**, *245*, 1–33. [[CrossRef](#)]
118. Sun, Y.; DeJaco, R.F.; Li, Z.; Tang, D.; Glante, S.; Sholl, D.S.; Colina, C.M.; Snurr, R.Q.; Thommes, M.; Hartmann, M. Fingerprinting Diverse Nanoporous Materials for Optimal Hydrogen Storage Conditions Using Meta-Learning. *Sci. Adv.* **2021**, *7*, eabg3983. [[CrossRef](#)]
119. Gangu, K.K.; Maddila, S.; Mukkamala, S.B.; Jonnalagadda, S.B. Synthesis, Structure, and Properties of New Mg(II)-Metal–Organic Framework and Its Prowess as Catalyst in the Production of 4H-Pyrans. *Ind. Eng. Chem. Res.* **2017**, *56*, 2917–2924. [[CrossRef](#)]
120. Gangu, K.K.; Dadhich, A.S.; Mukkamala, S.B. Synthesis, Crystal Structure and Fluorescent Properties of Two Metal–Organic Frameworks Constructed from Cd(II) and 2,6-Naphthalene Dicarboxylic Acid. *Inorg. Nano-Met. Chem.* **2017**, *47*, 313–319. [[CrossRef](#)]
121. Bétard, A.; Fischer, R.A. Metal–Organic Framework Thin Films: From Fundamentals to Applications. *Chem. Rev.* **2012**, *112*, 1055–1083. [[CrossRef](#)]
122. Sun, W.-F.; Sun, Y.-X.; Zhang, S.-T.; Chi, M.-H. Hydrogen Storage, Magnetism and Electrochromism of Silver Doped FAU Zeolite: First-Principles Calculations and Molecular Simulations. *Polymers* **2019**, *11*, 279. [[CrossRef](#)] [[PubMed](#)]
123. Silva, A.R.M.; Alexandre, J.Y.N.H.; Souza, J.E.S.; Neto, J.G.L.; de Sousa Júnior, P.G.; Rocha, M.V.P.; dos Santos, J.C.S. The Chemistry and Applications of Metal–Organic Frameworks (MOFs) as Industrial Enzyme Immobilization Systems. *Molecules* **2022**, *27*, 4529. [[CrossRef](#)]
124. Zhou, H.C.; Long, J.R.; Yaghi, O.M. Introduction to Metal–Organic Frameworks. *Chem. Rev.* **2012**, *112*, 673–674. [[CrossRef](#)] [[PubMed](#)]
125. Chen, Z.; Kirlikovali, K.O.; Idrees, K.B.; Wasson, M.C.; Farha, O.K. Porous Materials for Hydrogen Storage. *Chem* **2022**, *8*, 693–716. [[CrossRef](#)]
126. Gross, K.J.; Carrington, K.R.; Barcelo, S.; Karkamkar, A.; Purewal, J.; Ma, S.; Zhou, H.-C.; Dantzer, P.; Ott, K.; Pivak, Y. *Recommended Best Practices for the Characterization of Storage Properties of Hydrogen Storage Materials*; EMN-HYMARC (EMN-HyMARC); National Renewable Energy Lab. (NREL): Golden, CO, USA, 2016.
127. Akhtar, F.; Andersson, L.; Ogunwumi, S.; Hedin, N.; Bergström, L. Structuring Adsorbents and Catalysts by Processing of Porous Powders. *J. Eur. Ceram. Soc.* **2014**, *34*, 1643–1666. [[CrossRef](#)]
128. Ren, J.; North, B.C. Shaping Porous Materials for Hydrogen Storage Applications: A. *J. Technol.* **2014**, *3*, 13. [[CrossRef](#)]
129. Adhikari, A.K.; Lin, K.-S.; Tu, M.-T. Hydrogen Storage Capacity Enhancement of MIL-53(Cr) by Pd Loaded Activated Carbon Doping. *J. Taiwan Inst. Chem. Eng.* **2016**, *63*, 463–472. [[CrossRef](#)]
130. Musyoka, N.M.; Ren, J.; Annamalai, P.; Langmi, H.W.; North, B.C.; Mathe, M.; Bessarabov, D. Synthesis of a Hybrid MIL-101(Cr)/ZTC Composite for Hydrogen Storage Applications. *Res. Chem. Intermed.* **2016**, *42*, 5299–5307. [[CrossRef](#)]

131. Naeem, A.; Ting, V.P.; Hintermair, U.; Tian, M.; Telford, R.; Halim, S.; Nowell, H.; Holyńska, M.; Teat, S.J.; Scowen, I.J.; et al. Mixed-Linker Approach in Designing Porous Zirconium-Based Metal–Organic Frameworks with High Hydrogen Storage Capacity. *Chem. Commun.* **2016**, *52*, 7826–7829. [[CrossRef](#)]
132. Li, J.-P.; Ma, Y.-Q.; Geng, L.-H.; Li, Y.-H.; Yi, F.-Y. A Highly Stable Porous Multifunctional Co(Li) Metal–Organic Framework Showing Excellent Gas Storage Applications and Interesting Magnetic Properties. *CrystEngComm* **2015**, *17*, 6471–6475. [[CrossRef](#)]
133. Gómez-Gualdrón, D.A.; Moghadam, P.Z.; Hupp, J.T.; Farha, O.K.; Snurr, R.Q. Application of Consistency Criteria to Calculate BET Areas of Micro- and Mesoporous Metal–Organic Frameworks. *J. Am. Chem. Soc.* **2016**, *138*, 215–224. [[CrossRef](#)] [[PubMed](#)]
134. Chen, Z.; Mian, M.R.; Lee, S.-J.; Chen, H.; Zhang, X.; Kirlikovali, K.O.; Shulda, S.; Melix, P.; Rosen, A.S.; Parilla, P.A. Fine-Tuning a Robust Metal–Organic Framework toward Enhanced Clean Energy Gas Storage. *J. Am. Chem. Soc.* **2021**, *143*, 18838–18843. [[CrossRef](#)] [[PubMed](#)]
135. Lim, W.-X.; Thornton, A.W.; Hill, A.J.; Cox, B.J.; Hill, J.M.; Hill, M.R. High Performance Hydrogen Storage from Be-BTB Metal–Organic Framework at Room Temperature. *Langmuir* **2013**, *29*, 8524–8533. [[CrossRef](#)]
136. Gu, K.; Wei, F.; Cai, Y.; Lin, S.; Guo, H. Dynamics of Initial Hydrogen Spillover from a Single Atom Platinum Active Site to the Cu(111) Host Surface: The Impact of Substrate Electron–Hole Pairs. *J. Phys. Chem. Lett.* **2021**, *12*, 8423–8429. [[CrossRef](#)] [[PubMed](#)]
137. Conner, W.C.J.; Falconer, J.L. Spillover in Heterogeneous Catalysis. *Chem. Rev.* **1995**, *95*, 759–788. [[CrossRef](#)]
138. Shen, H.; Li, H.; Yang, Z.; Li, C. Magic of Hydrogen Spillover: Understanding and Application. *Green Energy Environ.* **2022**, *7*, 1161–1198. [[CrossRef](#)]
139. Zhang, X.; Zheng, Q.; He, H. Synergistic Effect of Hydrogen Spillover and Nano-Confined AlH₃ on Room Temperature Hydrogen Storage in MOFs: By GCMC, DFT and Experiments. *Int. J. Hydrog. Energy* **2023**, *in press*. [[CrossRef](#)]
140. Li, Y.; Yang, R.T. Significantly Enhanced Hydrogen Storage in Metal–Organic Frameworks via Spillover. *J. Am. Chem. Soc.* **2006**, *128*, 726–727. [[CrossRef](#)] [[PubMed](#)]
141. Li, Y.; Yang, R.T. Hydrogen Storage in Metal–Organic Frameworks by Bridged Hydrogen Spillover. *J. Am. Chem. Soc.* **2006**, *128*, 8136–8137. [[CrossRef](#)] [[PubMed](#)]
142. Sumida, K.; Horike, S.; Kaye, S.S.; Herm, Z.R.; Queen, W.L.; Brown, C.M.; Grandjean, F.; Long, G.J.; Dailly, A.; Long, J.R. Hydrogen Storage and Carbon Dioxide Capture in an Iron-Based Sodalite-Type Metal–Organic Framework (Fe-BTT) Discovered via High-Throughput Methods. *Chem. Sci.* **2010**, *1*, 184–191. [[CrossRef](#)]
143. Ibarra, I.A.; Yang, S.; Lin, X.; Blake, A.J.; Rizkallah, P.J.; Nowell, H.; Allan, D.R.; Champness, N.R.; Hubberstey, P.; Schröder, M. Highly Porous and Robust Scandium-Based Metal–Organic Frameworks for Hydrogen Storage. *Chem. Commun.* **2011**, *47*, 8304–8306. [[CrossRef](#)] [[PubMed](#)]
144. Gómez-Gualdrón, D.A.; Wang, T.C.; García-Holley, P.; Sawelewa, R.M.; Argueta, E.; Snurr, R.Q.; Hupp, J.T.; Yildirim, T.; Farha, O.K. Understanding Volumetric and Gravimetric Hydrogen Adsorption Trade-off in Metal–Organic Frameworks. *ACS Appl. Mater. Interfaces* **2017**, *9*, 33419–33428. [[CrossRef](#)]
145. Zhang, X.; Lin, R.; Wang, J.; Wang, B.; Liang, B.; Yildirim, T.; Zhang, J.; Zhou, W.; Chen, B. Optimization of the Pore Structures of MOFs for Record High Hydrogen Volumetric Working Capacity. *Adv. Mater.* **2020**, *32*, 1907995. [[CrossRef](#)] [[PubMed](#)]
146. Chen, Z.; Li, P.; Zhang, X.; Li, P.; Wasson, M.C.; Islamoglu, T.; Stoddart, J.F.; Farha, O.K. Reticular Access to Highly Porous Acs-MOFs with Rigid Trigonal Prismatic Linkers for Water Sorption. *J. Am. Chem. Soc.* **2019**, *141*, 2900–2905. [[CrossRef](#)]
147. Panella, B.; Hirscher, M.; Pütter, H.; Müller, U. Hydrogen Adsorption in Metal–Organic Frameworks: Cu-MOFs and Zn-MOFs Compared. *Adv. Funct. Mater.* **2006**, *16*, 520–524. [[CrossRef](#)]
148. Yan, X.; Komarneni, S.; Zhang, Z.; Yan, Z. Extremely Enhanced CO₂ Uptake by HKUST-1 Metal–Organic Framework via a Simple Chemical Treatment. *Microporous Mesoporous Mater.* **2014**, *183*, 69–73. [[CrossRef](#)]
149. Lin, K.-S.; Adhikari, A.K.; Ku, C.-N.; Chiang, C.-L.; Kuo, H. Synthesis and Characterization of Porous HKUST-1 Metal Organic Frameworks for Hydrogen Storage. *Int. J. Hydrog. Energy* **2012**, *37*, 13865–13871. [[CrossRef](#)]
150. Kim, J.; Shapiro, L.; Flynn, A. The Clinical Application of Mesenchymal Stem Cells and Cardiac Stem Cells as a Therapy for Cardiovascular Disease. *Pharmacol. Ther.* **2015**, *151*, 8–15. [[CrossRef](#)]
151. Gygi, D.; Bloch, E.D.; Mason, J.A.; Hudson, M.R.; Gonzalez, M.I.; Siegelman, R.L.; Darwish, T.A.; Queen, W.L.; Brown, C.M.; Long, J.R. Hydrogen Storage in the Expanded Pore Metal–Organic Frameworks M2(Dobpdc) (M = Mg, Mn, Fe, Co, Ni, Zn). *Chem. Mater.* **2016**, *28*, 1128–1138. [[CrossRef](#)]
152. Viditha, V.; Srilatha, K.; Himabindu, V. Hydrogen Storage Studies on Palladium-Doped Carbon Materials (AC, CB, CNMs) @ Metal–Organic Framework-5. *Environ. Sci. Pollut. Res.* **2016**, *23*, 9355–9363. [[CrossRef](#)] [[PubMed](#)]
153. Jaramillo, D.E.; Jiang, H.Z.H.; Evans, H.A.; Chakraborty, R.; Furukawa, H.; Brown, C.M.; Head-Gordon, M.; Long, J.R. Ambient-Temperature Hydrogen Storage via Vanadium (II)-Dihydrogen Complexation in a Metal–Organic Framework. *J. Am. Chem. Soc.* **2021**, *143*, 6248–6256. [[CrossRef](#)] [[PubMed](#)]

Disclaimer/Publisher’s Note: The statements, opinions and data contained in all publications are solely those of the individual author(s) and contributor(s) and not of MDPI and/or the editor(s). MDPI and/or the editor(s) disclaim responsibility for any injury to people or property resulting from any ideas, methods, instructions or products referred to in the content.